

## **Supplemental Material**

### **Uremic toxin indoxyl sulfate promotes pro-inflammatory macrophage activation via the interplay of OATB2B1 and DII4-Notch signaling**

#### **Potential mechanism for accelerated atherogenesis in chronic kidney disease**

Toshiaki Nakano, MD, PhD; Masanori Aikawa, MD, PhD, et al.

#### **Online materials and methods supplement**

The data, analytic methods, and study materials will be made available to other researchers upon request for purposes of reproducing the results or replicating the procedure. The data are available through <https://aikawalabs.bwh.harvard.edu/CKD>.

#### **Cell cultures**

Buffy coats were purchased from Research Blood Components, LLC (Boston, MA) and derived from de-identified healthy donors. The company recruits healthy donors under a New England Institutional Review Board-approved protocol for the Collection of White Blood for Research Purposes (NEIRB#04-144). We had no access to the information about donors. Human PBMC, isolated by density gradient centrifugation from buffy coats, were cultured in RPMI-1640 (Thermo Fisher Scientific, Waltham, MA) containing 5% human serum and 1% penicillin/streptomycin for 10 days to differentiate macrophages. In stimulation assays, confluent macrophages were rinsed extensively with PBS, starved for 24 hours in 1% serum media with or without 4% albumin (Sigma-Aldrich, St. Louis MO), and treated with indoxyl sulfate (Sigma-Aldrich) or tryptophan (Sigma-Aldrich). In inhibition assays, macrophages were starved for 24 hours and pretreated with TAK-242 (10  $\mu$ mol/L, Cayman chemical, Ann Arbor, MI) for 1 hour,  $\gamma$ -Secretase inhibitor (DAPT, 10  $\mu$ mol/L, Sigma-Aldrich) or DMSO (Sigma-Aldrich) for 6 hours; anti-human DII4 blocking antibody (MHD4-46, 10  $\mu$ g/mL) or isotype IgG for 24 hours; or Probenecid (10 mmol/L, Sigma-Aldrich), Rifampicin (100 $\mu$ M, Sigma-Aldrich)

or Cyclosporin A (10  $\mu\text{mol/L}$ , Sigma-Aldrich) for 30 minutes as in previous reports<sup>1-3</sup> before stimulation with indoxyl sulfate.

RAW264.7 cells (American Type Culture Collection, ATCC, Rockville, MD) were maintained in DMEM (Thermo Fisher Scientific) containing 10% fetal bovine serum (FBS). In stimulation assays, confluent macrophages were rinsed extensively with PBS, starved for 24 hours in 0.5% serum media and treated with indoxyl sulfate. All experiments of RAW264.7 cells were performed between 5 to 10 passages.

For degradation assays, macrophages were starved for 24 hours and treated with cycloheximide (100  $\mu\text{g/mL}$ , Sigma-Aldrich), MG132 (1.0  $\mu\text{mol/L}$ , Enzo Life Sciences, Farmigdale, NY) or chloroquine (10  $\mu\text{mol/L}$ , Sigma-Aldrich).

#### **Limulus amoebocyte lysate (LAL) endotoxin assay**

To measure the endotoxin level in the reagent of indoxyl sulfate, the chromogenic LAL endotoxin assay was performed (GenScript, Piscataway, NJ). The pH value of indoxyl sulfate was adjusted to 7.0 with endotoxin-free 0.1N sodium hydroxide, according to the manufacturer's instruction. The minimum endotoxin detection limit is 0.005 EU/mL.

#### **Liquid chromatography mass spectrometry analysis for indoxyl sulfate**

Mass spectrometric analysis of 10  $\mu\text{mol/L}$  indoxyl sulfate was performed on the Thermo Q Exactive Plus Orbitrap mass spectrometer with a Thermo/Dionex Ultimate 3000 uHPLC (Thermo Fisher Scientific) in positive and negative ionization modes at Small Molecules Mass Spectrometry, a Harvard FAS Division of Science Core Facility, Harvard University.

#### **Tandem mass tagging (TMT) sample preparation and liquid chromatography tandem mass spectrometry (LC-MS/MS)**

We stimulated RAW264.7 cells with or without 1.0 mM indoxyl sulfate, and cells were

collected at 0 min, 15 min, 30 min, 1 hr and 3 hrs. Each time point was a pool of two well replicates, in order to average the biological/plate-to-plate variation. Cells from each condition were lysed with RIPA buffer containing 1% halt protease inhibitor cocktail and proteolysed (Lys-C, Wako Chemicals) using in-solution urea strategy detailed previously<sup>4</sup>. Peptides were labeled with TMT 10-plex reagent (Pierce). The reporter ion channels were assigned as follows:

without indoxyl sulfate - 126 (0 min), 127N (15 min), 127C (30 min), 128N (1 hr) and 128C (3 hr); and with indoxyl sulfate – 129N (0 min), 129C (15 min), 130N (30 min), 130C (1 hr) and 131 (3 hr). The labeled peptides were combined and desalted using Oasis Hlb 1cc columns (Waters). The peptides were then fractionated into 24 fractions based on their isoelectric focusing point (pH range of 3-10) using the OFF-gel system (Agilent). The fractions were dried using a tabletop speed vacuum, cleaned with the Oasis columns and resuspended in 40  $\mu$ l of 5% acetonitrile and 5% formic acid for subsequent analysis by liquid chromatography/mass spectrometry (LC/MS).

The high resolution/accuracy Orbitrap Fusion Lumos mass spectrometer (Thermo Scientific) was used to analyze the TMT peptide samples. The analytical gradient was run at 300 nl/min from 5 to 21% Solvent B (acetonitrile/0.1 % formic acid) for 75 minutes, 21 to 30 % Solvent B for 15 minutes, followed by five minutes of 95 % Solvent B. Solvent A was 0.1 % formic acid. The precursor scan was set to 120 K resolution, and the top N precursor ions in 3 seconds cycle time (within a scan range of 375-1500 m/z) were subjected to higher energy collision induced dissociation (HCD, collision energy 38%, isolation width 0.7 m/z, dynamic exclusion enabled, starting m/z fixed at 100 m/z, and resolution set to 50 K) for peptide sequencing (MS/MS). The MS/MS data were queried against the mouse UniProt database (downloaded on August 1, 2014) using the SEQUEST search algorithm, via the Proteome Discoverer (PD) Package (version 2.1, Thermo Scientific), using a 10 ppm tolerance window in the MS1 search space, and a 0.02 Da fragment tolerance window for

HCD. Methionine oxidation was set as a variable modification, and carbamidomethylation of cysteine residues and 10-plex TMT tags (Thermo Scientific) were set as fixed modifications. The peptide false discovery rate (FDR) was calculated using Percolator provided by PD: the FDR was determined based on the number of MS/MS spectral hits when searched against the reverse, decoy human database. Peptides were filtered based on a 1% FDR. Peptides assigned to a given protein group, and not present in any other protein group, were considered as unique. Consequently, each protein group is represented by a single master protein (PD Grouping feature). Master proteins with two or more unique peptides were used for TMT reporter ratio quantification. The normalized and scaled reporter ion intensities were exported from PD2.1 the analysis below.

### **Proteomics data clustering**

Quantitative proteomics analyses were done using the R (version 3.3.2) and our previously published software for high-dimensional quantitative proteomics analysis <sup>5</sup>. First, we determined the indoxyl sulfate-dependent response of the proteome by calculating the ratio of indoxyl sulfate / control, at every time point (0, 15, 30, 60 and 180 minutes), followed by a reference normalization using the 0 minute time point <sup>6</sup>. The protein abundance profiles were then sum-normalized <sup>6</sup> and clustered by their expression pattern using Model-based clustering <sup>5, 6</sup>.

### **Pathway enrichment analysis and pathway networks**

Using ConsensusPathDB <sup>7</sup>, the gene sets corresponding to each cluster were tested for enrichment by a hypergeometric test and adjusted for multiple comparisons using the Benjamini-Hochberg method for controlling false discovery rate (FDR). For the pathway enrichment analysis (pathway data retrieved from <http://consensuspathdb.org/> in October 2017), pathways with FDR adjusted p-value (q-value) < 0.05 were considered as

significantly enriched. The pathway networks consist of pathways as the nodes and the shared genes between pathways as the edges. Node size corresponds to  $-\log(q\text{-value})$  and edge weight (thickness) corresponds to the gene overlap between pairs of pathways measured by the Jaccard index  $J$ , which is defined as

$$J = \frac{s_A \cap s_B}{s_A \cup s_B}$$

where  $s_A$  and  $s_B$  are the set of proteins detected in proteomics that belong to pathway  $A$  and pathway  $B$ , respectively. Edges with a Jaccard index  $< 0.1$  were discarded in the visualization for clarity. The network visualizations were made using Gephi v0.8.2.

### **Network closeness to human diseases**

The first neighbor networks were built by taking the direct interaction partners of the proteins in the respective cluster that have a fold-change greater than 1.5 between 0 minutes and 30 minutes. The closeness of the first neighbor networks to disease proteins was measured in terms of the average shortest distance. The average shortest distance  $D$  to disease genes in a module was measured by calculating the shortest distance between each first neighbor network gene  $s$  and all disease genes  $t$  and then averaging over all first neighbor network genes such that

$$d_s = \frac{1}{N_T} \sum_{t \in \mathbb{T}} d_{st}$$

and

$$D = \frac{1}{N_S} \sum_{s \in \mathbb{S}} d_s$$

where  $d_{st}$  is the shortest network (non-Euclidean) distance between  $s$  and  $t$ ,  $\mathbb{S}$  and  $\mathbb{T}$  are the set of genes in the first neighbor network and disease genes, respectively, and  $N_S$  and  $N_T$  are the number of genes in these sets. In order to compare this average shortest distance value to a random expectation, the average shortest distance of the same number of randomly selected genes to disease genes was calculated for  $N=100$  realizations. To correct

for degree (i.e., the number of connections of a gene) bias, the random selection was done in a degree-preserving manner where all genes were binned according to their degree and random genes were selected uniformly at random from their corresponding degree bin.

Empirical p-values were calculated by

$$p_{emp.} = P(D_r < D)$$

where  $D_r$  is the average shortest distance of a randomized instance,  $\langle D_r \rangle$  is the mean of the average shortest distance of all randomized instances, and  $\sigma_{D_r}$  is their standard deviation. The disease genes were obtained from the DiseaseConnect (<http://disease-connect.org>)<sup>8</sup> (using entries with evidence from Genome-Wide Association Studies (GWAS) and Online Mendelian Inheritance in Man (OMIM) (<http://www.omim.org/>)) and MalaCards (<http://www.malacards.org/>)<sup>9</sup> databases, for a range of diseases including cardiovascular, metabolic, malignant, and auto-immune disorders. The underlying protein-protein interaction (PPI) network onto which genes were mapped consists of curated physical protein-protein interactions with experimental support, including binary interactions, protein complexes, enzyme-coupled reactions, signaling interactions, kinase-substrate pairs, regulatory interactions and manually curated interactions from literature, the details of which were described previously<sup>10</sup>. The PPI network was treated as undirected, due to the limited availability of unambiguous and robust information on the directionality of links in the available datasets. Network measures including shortest distances and centralities were calculated using the NetworkX package v1.9 in Python v2.7.10.

### **Isolation of mouse primary macrophages from peritoneal cells**

Peritoneal cells were collected after injection of PBS with 1% FBS into the mouse peritoneal cavity. F4/80 positive macrophages were isolated by magnetic sorting (EasySep system, StemCell Technologies, Cambridge, MA). PE-conjugated anti-F4/80 antibody (Biolegend, San Diego, CA) was used as the primary antibody to specifically select macrophages.

### **RNA interference in cultured cells**

In siRNA experiments, human primary macrophages or mouse peritoneal macrophages were transfected with 20 nmol/L siRNA using SilenceMag (BOCA Scientific, Boca Raton, FL), according to the manufacturer's instruction. Macrophages were stimulated with indoxyl sulfate after 48 hours from transfection. siRNA against human DLL4 (L-010490), human SLCO2B1 (L-007442), SLCO3A1 (L-007434), SLCO4A1 (L-007435), SLCO1A2 (L-007439), SLCO5A1 (L-007437), SLCO6A1 (L-007353), SLCO22A10 (L-029855), SLCO22A11 (L-0007445), SLCO22A20 (L-032385), TLR2 (L-005120), TLR4 (L-008088), USP5 (L-006095), USP7 (L-006097), USP14 (L-006065), USP48 (L-006079) and non-target (D-001810) were all ON-TARGETplus SMARTpool, purchased from GE Dharmacon (Lafayette, CO). siRNA against mouse Slco2b1 (XD-07161) and luciferase control (XD-00194) were purchased from Axolabs (Kulmbach, Germany). siRNA against mouse Dll4 was a generous gift of Alnylam Pharmaceuticals (Cambridge, MA).

### **Reverse transcription, quantitative real-time PCR and semi-quantitative PCR**

RNA was extracted from cells by illustra RNAspin Mini kit (GE Healthcare, Little Chalfont, UK), or tissues by Trizol (Thermo Fisher Scientific). cDNA was synthesized by High Capacity cDNA Reverse Transcription Kit (Applied Biosystems, Waltham, MA). Quantitative real-time PCR was performed with a 7900HT Fast Real-Time PCR System (Applied Biosystems) or a CFX Connect Real-Time PCR Detection System (Bio-Rad, Hercules, CA). Primer designs are listed on **supplemental table 1 and 3**. Data were calculated by  $\Delta\Delta CT$  method and expressed in arbitrary units that were normalized by  $\beta$ -actin or GAPDH. Semi-quantitative PCR was performed with a T100 Thermal Cycler (Bio-Rad), and primer designs are listed on **supplemental table 2**. All experiments of PCR were performed in duplicate for technical replicate.

### **Flow cytometry**

Human peripheral blood mononuclear cells were cultured for 10 days and differentiated to macrophages. Human macrophages were starved for 24 hours in 1% serum media and incubated with indoxyl sulfate. The cells were treated with 2mM EDTA, suspended in PBS, and fixed with 5% formaldehyde. The cells were washed with a MACS buffer (Miltenyi Biotec, Bergisch Gladbach, Germany) and incubated with human Fc block (BD Biosciences, Franklin Lakes, NJ), followed by PE anti-human Delta-like protein 4 antibody (MHD4-46, BioLegend, San Diego, CA) or isotype control. After washing, the cell were subjected to the flow cytometer (BD Fortessa, BD Biosciences). Data were analyzed with FlowJo v.10 (Tree Star, Inc., Ashland, OR)

### **RBP-Jk luciferase reporter assay**

RAW264.7 cells were transfected with RBP-Jk reporter (Signal reporter assay kit, Qiagen, Hilden, Germany) by electroporation (Nucleofector system, Lonza, Basel, Switzerland), according to the manufacturer's instructions. We transfected 1µg plasmid to cells and incubate for 24 hours, followed by incubation with 0.5 mmol/L indoxyl sulfate for 24 hours. Luciferase activity was determined using a Dual-Luciferase Reporter Assay System (Promega, Fitchburg, WI).

### **Quantification of indoxyl sulfate**

Human primary macrophages were cultured in 6-well plates for 10 days and treated with Probenecid (10 mmol/L), Rifampicin (100µmol/L) or Cyclosporin A (10 µmol/L) for 30 minutes before stimulation with indoxyl sulfate. About SLCO2B1 siRNA, macrophages were stimulated with indoxyl sulfate after 48 hours from transfection. Macrophages were stimulated with 2 mmol/L indoxyl sulfate for 30 minutes (Probenecid, Rifampicin, Cyclosporin



A) or 15 minutes (SLCO2B1 siRNA). The cells were washed by PBS twice and ice-cold NaOH (0.2 mol/L, 100 $\mu$ L) was added to each well and the plates were placed in a refrigerator for at least one hour to lyse the cells <sup>2</sup>. The cell homogenate was neutralized with an equal volume of HCl (0.2 mol/L). Protein concentration was determined by BCA assay. Indoxyl sulfate concentrations in cell lysate or mouse plasma were measured by HPLC. HPLC analysis of 20  $\mu$ g cell lysate or 20  $\mu$ L aliquot of plasma were performed using Shimadzu HPLC system (prominence series) consisted of an Inertsil column (ODS-3, 5 $\mu$ m, 4.0x150mm) and a UV detector (280nm).

### **Western blot analysis**

Total cellular protein was collected from cells at 4 $^{\circ}$ C in RIPA buffer (Thermo Fisher Scientific) containing 1% halt protease inhibitor cocktail (Thermo Fisher Scientific) and phosphatase inhibitor cocktail (PhosSTOP, Roche). Protein concentration was determined by BCA assay and 50  $\mu$ g protein was loaded onto each lane. Blots were stained with anti-Cleaved Notch1 antibody (Val1744, Cell Signaling Technology, Danvers, MA), anti-Dll4 antibody (Rockland, Limerick, PA, and Cell Signaling Technology), anti-SLCO2B1 antibody (LifeSpan BioSciences, Inc., Seattle, WA), anti-USP5 antibody (ab154170, Abcam, Cambridge, MA) and anti- $\beta$ Actin antibody (Cell Signaling Technology).

### **CyTOF Analysis**

Human PBMCs were cultured for 10 days and differentiated into macrophages. Human macrophages were starved for 24 hours in 1% serum media and incubated with 1mmol/L indoxyl sulfate for 48 hours. The cells were detached with Accutase Cell Detachment Solution (BD Biosciences). Dead cells were stained using Cell-ID Cisplatin (Fluidigm, San Francisco, CA). The cells were stained with anti-Dll4 antibody (Rockland, Metal isotope 150Nd), anti-CD68 antibody (Y1/82A, 171Yb), anti-CD163 antibody (GJI/61, 165Ho) and

anti-CD206 antibody (15-2, 168Er) for 30 minutes, then washed, fixed with Fix I buffer (Fluidigm), incubated with Fix and Perm Buffer (Fluidigm), permeabilized with Perm S Buffer (Fluidigm) and stained with anti-TNF- $\alpha$  antibody (Mab11, 144Nd), anti-MCP-1 antibody (2H5, 147Sm) for 30 minutes. The cells were stained with Intercalator Ir (Fluidigm), then washed, and resuspended in distilled water containing EQ Four Element Calibration Beads (Fluidigm). Samples were measured by CyTOF Mass Cytometer-039-Helios (Fluidigm), and the data were uploaded to Cytobank and analyzed by SPADE using clustering channels of DII4, CD68, CD163, CD206, TNF- $\alpha$  and MCP-1. The result were pre-gated to exclude EQ beads, cell debris, cell doublets and dead cells.

### **Osteoclast experiments**

For osteoclast-like differentiation experiments, RAW264.7 cells were cultured overnight at  $2.0 \times 10^4$  cells/cm<sup>2</sup> in 10% FBS containing Minimum Essential Medium Eagle alpha modified media ( $\alpha$ -MEM, Gibco) supplemented with penicillin and streptomycin. These cells were incubated with 50 ug/mL of Hamster IgG (BioXcell, cat#BE0091) or mouse DII4 Ab (BioXcell HMD4-2, cat#BE0127) immediately followed by stimulation with or without 100 ng/mL of recombinant mouse RANKL (Peprotech, cat#315-11). Two or three days after stimulation, RANKL-treated RAW264.7 cells had a phenotype similar to osteoclasts as assessed by TRAP staining (Cosmo Bio, cat#PMC-AK04F-COS). TRAP staining was performed according to the manufacturer's protocol. TRAP stained cell images were photographed using Eclipse TE2000-U microscope (Nikon) with INFINITY3 camera and INFINITY CAPTURE Software (Lumenera, Ontario, Canada) at 20X magnification.

## **5/6 nephrectomy in mice**

Male *Ldlr*<sup>-/-</sup> mice with C57BL/6 background were fed a high-fat diet (HFD) containing 1.25% cholesterol (D12108; Research Diets, NJ) from 8 weeks of age. To create 5/6 nephrectomy in mice (CKD mice), we used a well-established two-step procedure of 5/6 nephrectomy<sup>11</sup>,<sup>12</sup>. Our laboratory has used this procedure previously<sup>13</sup><sup>14</sup>. Mice were anesthetized by isoflurane inhalation and received Buorenorphine (0.1mg/kg) subcutaneously for a preemptive analgesia. The first step involved a semi-nephrectomy of the left kidney (removal of 2/3 of the left kidney) in mice of the CKD Group (n=20) at 10 weeks of age. The CKD Group were subjected to a right nephrectomy a week later at 11 weeks of age. Mice of the Control Group underwent a sham operation at 10 and 11 weeks of age. The mice of Control Group (n=20) and CKD Groups continued on HCD for 16 weeks. For the selective blockade of Dll4, we intraperitoneally administered hamster anti-mouse Dll4 antibody (250 µg per injection) or control IgG twice a week. After 16 weeks, atherosclerotic lesions were evaluated. All animal experiments were approved by the BWH Animal Welfare Assurance (protocol 2016N000219).

## **Administration of Dll4 antibody or macrophage-targeted lipid nanoparticles**

Indoxyl sulfate of 100 mg/kg/day was intraperitoneally injected to 8-week old C57BL/6 mice every day for a week. Hamster anti-mouse Dll4 antibody (10 µg/g per injection) or control IgG were also injected twice a week. *Slco2b1* siRNA, Dll4 siRNA and control siRNA targeting luciferase were encapsulated in macrophage-targeted C12-200 lipid nanoparticles, as previously described<sup>15, 16</sup>. Macrophage-targeted lipid nanoparticles were prepared and mixed with siRNA to prepare siRNA encapsulated lipid nanoparticles<sup>15, 16</sup>. Lipid nanoparticles of 0.5 mg/kg were injected via tail vein to 8-week old C57BL/6 mice twice a week. Peritoneal macrophages were collected and isolated by magnetic sorting.

## **Histological analyses**

Human primary macrophages were washed with PBS and fixed with 10% neutral buffered formalin for 10 minutes, and subsequently washed and blocked with 1% skim milk in PBS. The slides were incubated with anti-Dll4 antibody (rabbit IgG, Rockland) and anti-CD68 (FITC-labeled, BD Biosciences) at 4°C overnight. Alexa Fluor anti-rabbit 568-labeled secondary antibody (Thermo Fisher Scientific) were subsequently applied. Nuclear staining with DAPI (Thermo Fisher Scientific) was performed.

Before isolation of the mouse aorta, we perfused 0.9% sodium chloride solution at a constant pressure via left ventricle. The thoracic aorta and aortic root were embedded in OCT compound (tissue Tek). Aortic tissues and valve tissues were sectioned serially (6µm) and stained with hematoxylin and eosin (H&E) staining for general morphology.

Immunohistochemistry by the avidin-biotin complex method employed anti-Mac3 (BD Biosciences). Immunofluorescence for Mac3 and Notch 1ICD was stained with anti-Mac3 (rat IgG1k, BD Biosciences) and anti-Notch 1ICD (rabbit IgG, Millipore), and subsequently stained with Alexa Fluor anti-rat 568-labeled secondary antibody and Alexa Fluor anti-rabbit 488-labeled secondary antibody (Thermo Fisher Scientific). Immunofluorescence for Mac3 and Dll4 was stained with anti-Mac3 (rat IgG1k, BD Biosciences) and anti-Dll4 (rabbit IgG, Abcam), and subsequently stained with Alexa Fluor anti-rat 488-labeled secondary antibody and Alexa Fluor anti-rabbit 568-labeled secondary antibody (Thermo Fisher Scientific).

Alkaline phosphatase (ALP) activity was detected, according to the manufacturer's instructions (alkaline phosphatase substrate kit, Vector Laboratories).

## **Ex vivo fluorescence reflectance imaging of the aorta and heart**

Bisphosphonate-conjugated imaging agent (OsteoSense680 EX, PerkinElmer, Boston, MA) elaborates fluorescence evident through the near-infrared window (680 nm) detected osteogenic activity as previous described<sup>17, 18</sup>. Signals from osteogenic activity were

detected on hearts and aortas using the Kodak Imaging Station 4000MM Pro (Kodak).

### **Blood biochemical analysis**

Blood was collected from the heart and spun in a refrigerated centrifuge, and serum was stored at -80°C. Serum levels of urea, creatinine, phosphate and calcium were assessed by QuantiChrom assay kits (BioAssay Systems, Hayward, CA). Serum levels of total cholesterol, triglyceride were also assessed by each assay kit (Wako, Osaka, Japan).

### **Blood pressure measurement**

Blood pressure of each conscious mouse was measured with a non-invasive blood pressure system (CODA, Kent Scientific Corporation, Torrington, CT). In each mouse, the mean value of five measurements was used for comparison.

### **Statistical analysis**

Data are expressed as mean  $\pm$  SEM for continuous variables. Comparisons between two groups were performed with the unpaired Student's t-test. Comparisons of multiple groups were analyzed with one-way ANOVA followed by Tukey's post-hoc test, or two-way ANOVA followed by the Bonferroni test. Analyses were performed using SPSS Statistics 22 (IBM) and GraphPad Prism 7.0 (GraphPad Software). P values of <0.05 were considered statistically significant.

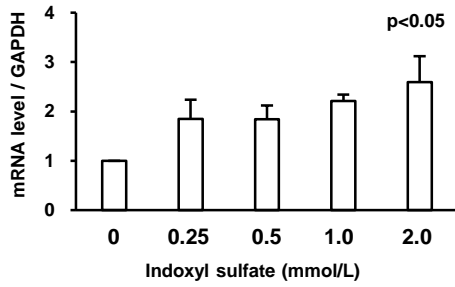
### **References**

1. Le Vee M, Jouan E, Stieger B, Fardel O. Differential regulation of drug transporter expression by all-trans retinoic acid in hepatoma HepaRG cells and human hepatocytes. *Eur J Pharm Sci.* 2013;48:767-774.
2. Brannstrom M, Nordell P, Bonn B, Davis AM, Palmgren AP, Hilgendorf C, Rubin K, Grime K. Montelukast Disposition: No Indication of Transporter-Mediated Uptake in OATP2B1 and

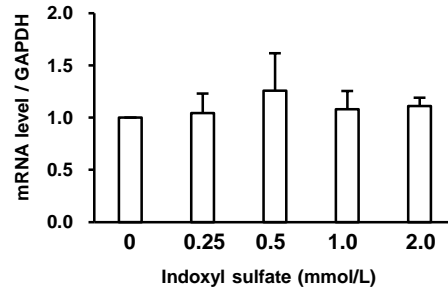
- OATP1B1 Expressing HEK293 Cells. *Pharmaceutics*. 2015;7:554-564.
3. Jeong HU, Kwon M, Lee Y, Yoo JS, Shin DH, Song IS, Lee HS. Organic anion transporter 3- and organic anion transporting polypeptides 1B1- and 1B3-mediated transport of catalposide. *Drug Des Devel Ther*. 2015;9:643-653.
  4. Iwata H, Goettsch C, Sharma A, Ricchiuto P, Goh WW, Halu A, Yamada I, Yoshida H, Hara T, Wei M, Inoue N, Fukuda D, Mojcher A, Mattson PC, Barabasi AL, Boothby M, Aikawa E, Singh SA, Aikawa M. PARP9 and PARP14 cross-regulate macrophage activation via STAT1 ADP-ribosylation. *Nat Commun*. 2016;7:12849.
  5. Ricchiuto P, Iwata H, Yabusaki K, Yamada I, Pieper B, Sharma A, Aikawa M, Singh SA. mIMT-visHTS: A novel method for multiplexing isobaric mass tagged datasets with an accompanying visualization high throughput screening tool for protein profiling. *J Proteomics*. 2015;128:132-140.
  6. Kirchner M, Renard BY, Kothe U, Pappin DJ, Hamprecht FA, Steen H, Steen JA. Computational protein profile similarity screening for quantitative mass spectrometry experiments. *Bioinformatics*. 2010;26:77-83.
  7. Kamburov A, Pentchev K, Galicka H, Wierling C, Lehrach H, Herwig R. ConsensusPathDB: toward a more complete picture of cell biology. *Nucleic Acids Res*. 2011;39:D712-717.
  8. Liu CC, Tseng YT, Li W, Wu CY, Mayzus I, Rzhetsky A, Sun F, Waterman M, Chen JJ, Chaudhary PM, Loscalzo J, Crandall E, Zhou XJ. DiseaseConnect: a comprehensive web server for mechanism-based disease-disease connections. *Nucleic Acids Res*. 2014;42:W137-146.
  9. Rappaport N, Nativ N, Stelzer G, Twik M, Guan-Golan Y, Stein TI, Bahir I, Belinky F, Morrey CP, Safran M, Lancet D. MalaCards: an integrated compendium for diseases and their annotation. *Database (Oxford)*. 2013;2013:bat018.
  10. Menche J, Sharma A, Kitsak M, Ghiassian SD, Vidal M, Loscalzo J, Barabasi AL. Disease networks. Uncovering disease-disease relationships through the incomplete interactome. *Science*. 2015;347:1257601.
  11. Gagnon RF, Duguid WP. A reproducible model for chronic renal failure in the mouse. *Urol Res*. 1983;11:11-14.
  12. Massy ZA, Ivanovski O, Nguyen-Khoa T, Angulo J, Szumilak D, Mothu N, Phan O, Daudon M, Lacour B, Druke TB, Muntzel MS. Uremia accelerates both atherosclerosis and arterial calcification in apolipoprotein E knockout mice. *J Am Soc Nephrol*. 2005;16:109-116.
  13. Aikawa E, Aikawa M, Libby P, Figueiredo JL, Rusanescu G, Iwamoto Y, Fukuda D, Kohler RH, Shi GP, Jaffer FA, Weissleder R. Arterial and aortic valve calcification abolished by elastolytic cathepsin S deficiency in chronic renal disease. *Circulation*. 2009;119:1785-1794.
  14. Figueiredo JL, Aikawa M, Zheng C, Aaron J, Lax L, Libby P, de Lima Filho JL, Gruener S, Fingerle J, Haap W, Hartmann G, Aikawa E. Selective cathepsin S inhibition attenuates atherosclerosis in apolipoprotein E-deficient mice with chronic renal disease. *Am J Pathol*. 2015;185:1156-1166.
  15. Leuschner F, Dutta P, Gorbatov R, Novobrantseva TI, Donahoe JS, Courties G, Lee KM, Kim JI, Markmann JF, Marinelli B, Panizzi P, Lee WW, Iwamoto Y, Milstein S, Epstein-Barash H, Cantley

- W, Wong J, Cortez-Retamozo V, Newton A, Love K, Libby P, Pittet MJ, Swirski FK, Koteliansky V, Langer R, Weissleder R, Anderson DG, Nahrendorf M. Therapeutic siRNA silencing in inflammatory monocytes in mice. *Nat Biotechnol.* 2011;29:1005-1010.
16. Koga J, Nakano T, Dahlman JE, Figueiredo JL, Zhang H, Decano J, Khan OF, Niida T, Iwata H, Aster JC, Yagita H, Anderson DG, Ozaki CK, Aikawa M. Macrophage Notch Ligand Delta-Like 4 Promotes Vein Graft Lesion Development: Implications for the Treatment of Vein Graft Failure. *Arterioscler Thromb Vasc Biol.* 2015;35:2343-2353.
  17. Aikawa E, Nahrendorf M, Sosnovik D, Lok VM, Jaffer FA, Aikawa M, Weissleder R. Multimodality molecular imaging identifies proteolytic and osteogenic activities in early aortic valve disease. *Circulation.* 2007;115:377-386.
  18. Fukuda D, Aikawa E, Swirski FK, Novobrantseva TI, Kotelianski V, Gorgun CZ, Chudnovskiy A, Yamazaki H, Croce K, Weissleder R, Aster JC, Hotamisligil GS, Yagita H, Aikawa M. Notch ligand delta-like 4 blockade attenuates atherosclerosis and metabolic disorders. *Proc Natl Acad Sci U S A.* 2012;109:E1868-1877.

### ABCG1

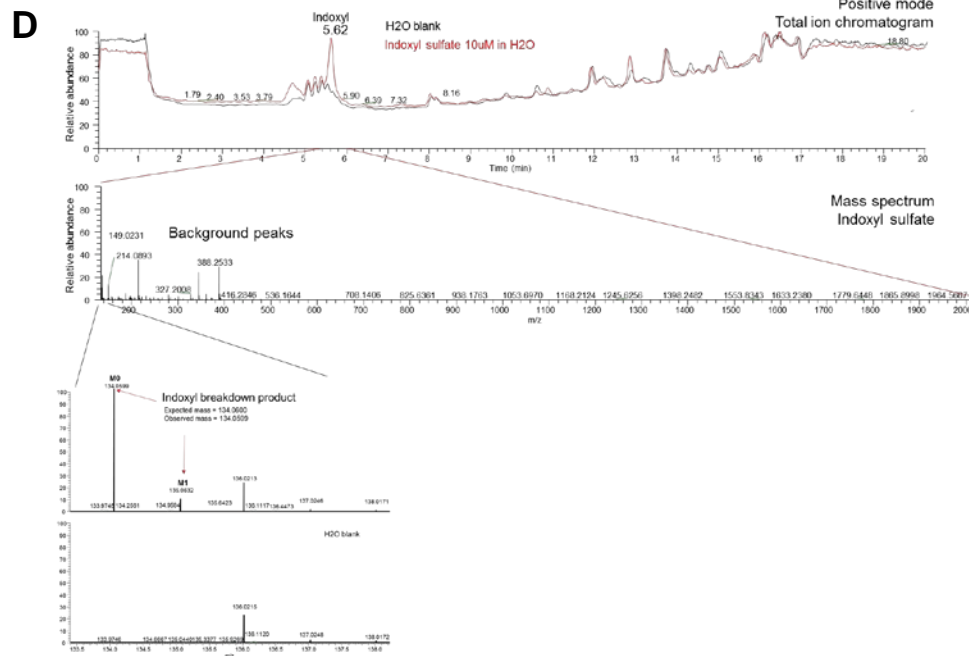
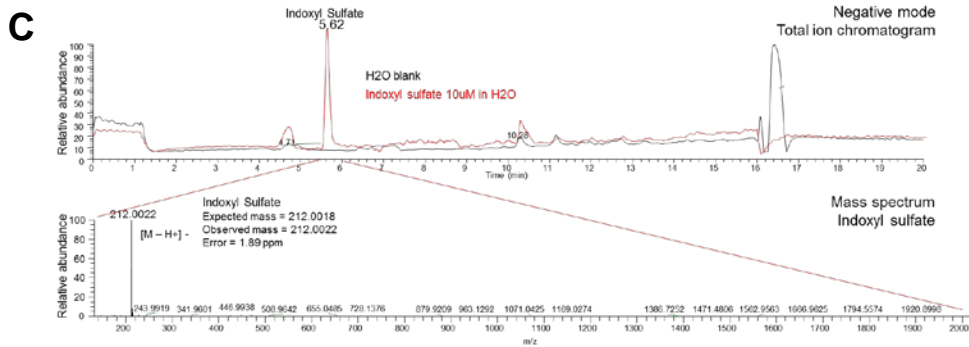
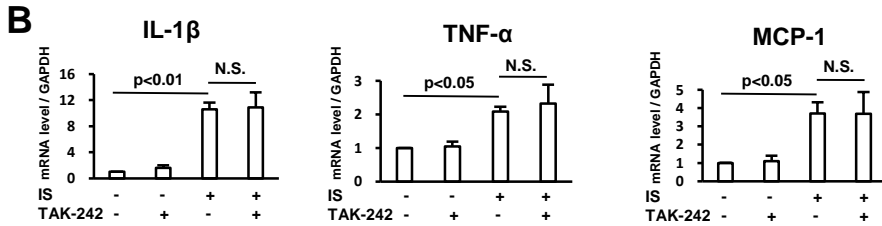
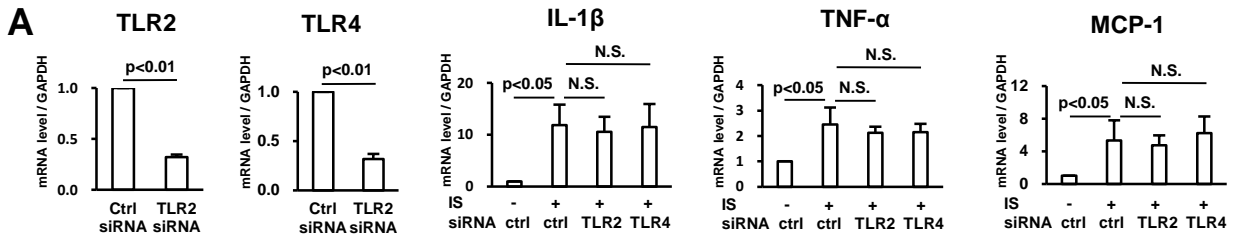


### ABCA1

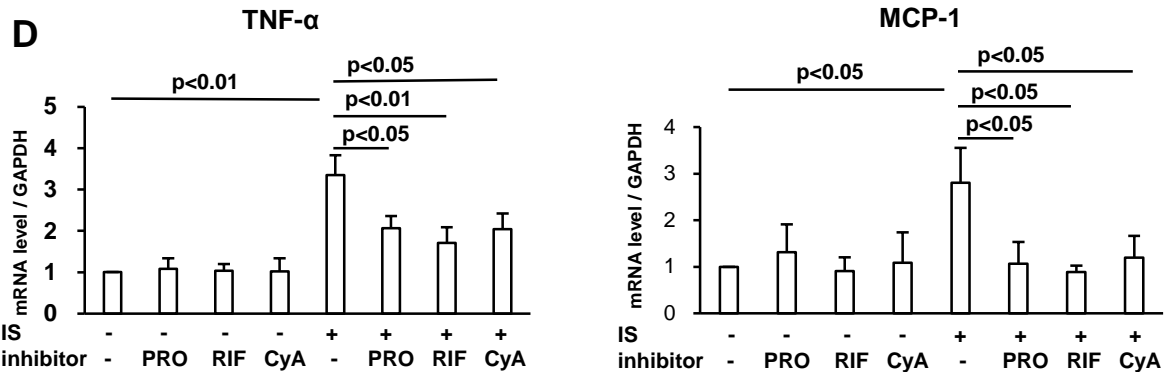
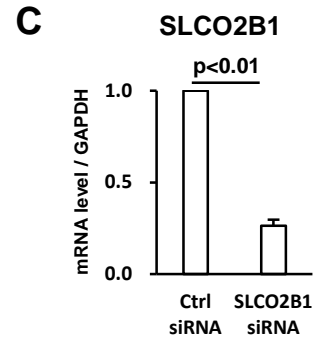
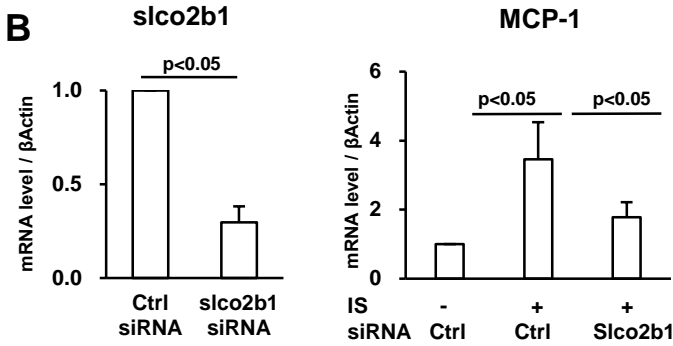
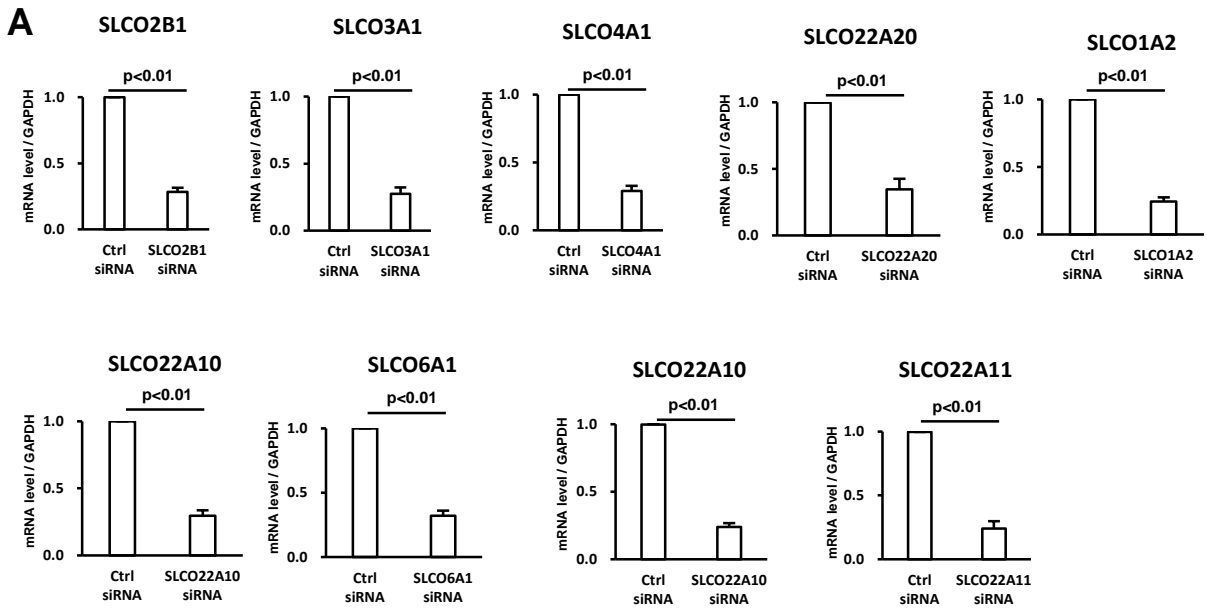


**Supplemental Figure 1. Indoxyl sulfate did not suppress ABCG1 and ABCA1 expression in human primary macrophages.** mRNA expression of ABCG1 and ABCA1 was measured in human primary macrophages after stimulation with indoxyl sulfate for 3 hours (7 PBMC donors). P value was calculated by one-way ANOVA followed by Tukey's test. Error bars indicate  $\pm$  SEM.

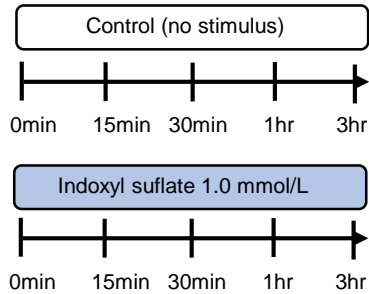
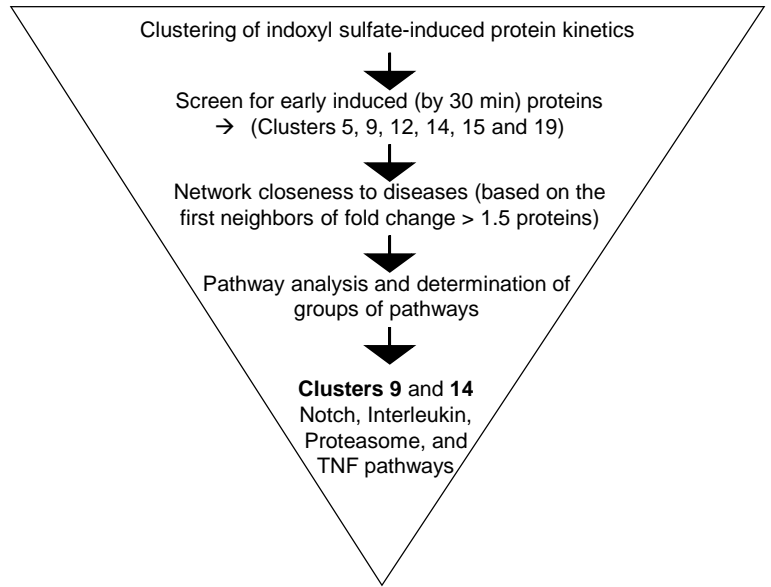




**Supplemental Figure 2. No evidence for contamination in indoxyl sulfate.** (A) mRNA expression was measured in human primary macrophages after pretreatment with TLR2 siRNA, TLR4 siRNA or control siRNA (ctrl) for 48 hours and stimulation with 0.5 mmol/L indoxyl sulfate (IS) for 3 hours (8 PBMC donors). (B) mRNA expression was measured in human primary macrophages after pretreatment with TLR inhibitor TAK-242 10nmol/L for 1 hour and stimulation with 0.5 mmol/L IS for 3 hours (8 donors). P value was calculated by unpaired Student's t-test or one-way ANOVA followed by Tukey's test. Error bars indicate  $\pm$  SEM. N.S., not-significant difference. (C,D) Liquid chromatography-mass spectrometry analysis indicates no contamination in the indoxyl sulfate reagent. Chromatogram and mass spectrum of indoxyl sulfate analyzed in positive ion mode (C). All peaks but that of indoxyl sulfate were detected in the water blank (C). Chromatogram and mass spectrum of indoxyl sulfate analyzed in negative ion mode (D). All peaks but that of indoxyl sulfate and its breakdown product (indoxyl) were detected in the water blank (D). Due to the identical retention time property of the sulfate derivative, the indoxyl ion (decay product) was likely generated in the mass spectrometer (D).

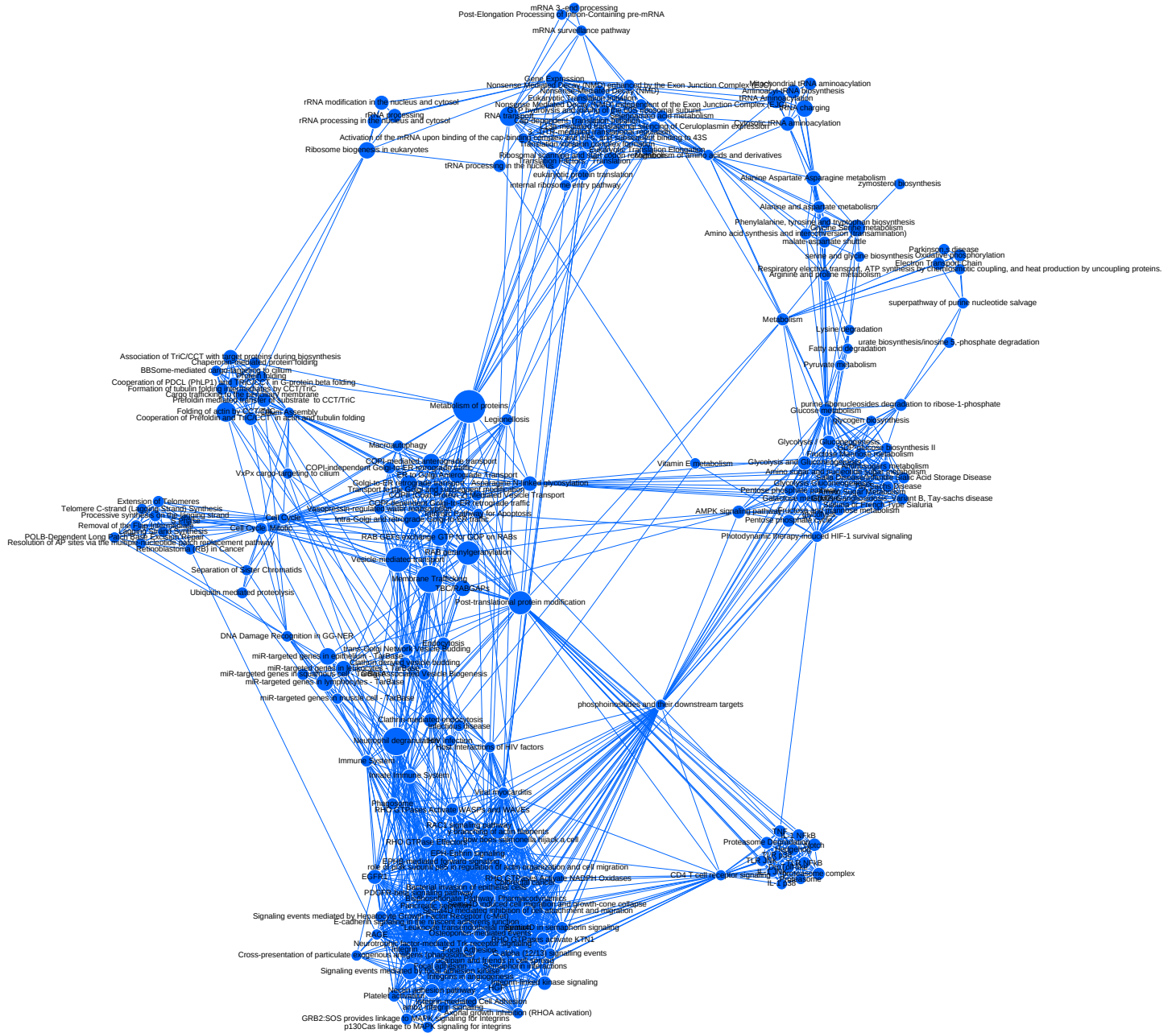


**Supplemental Figure 3. Inhibition of the uptake of indoxyl sulfate in macrophages.** (A) mRNA expression of OATs / OATPs in Figure 2B was measured in human primary macrophages after suppression by siRNA for 48 hours and stimulation with 0.5 mmol/L indoxyl sulfate (IS) for 3 hours (9 donors). (B) mRNA expression was measured in mouse peritoneal macrophages after suppression by siRNA for 48 hours and stimulation with 0.5 mmol/L IS for 3 hours (n=6). (C) mRNA expression of SLCO2B1 was measured in human primary macrophages in the presence of SLCO2B1 siRNA or control siRNA (6 donors). (D) mRNA expression of TNF- $\alpha$  and MCP-1 was measured after pretreatment with the OAT/OATP inhibitor 10 mmol/L probenecid (PRO), 100  $\mu$ mol/L rifampicin (RIF) and 10  $\mu$ mol/L cyclosporin A (CyA) for 30 minutes, and stimulation with 0.5 mmol/L IS for 3 hours (8 donors). P value was calculated by unpaired Student's t-test or one-way ANOVA followed by Tukey's test. Error bars indicate  $\pm$  SEM.

**A****Conditions and time points for proteomics****B**

**Supplemental Figure 4. Global proteomics and pathway network analysis of the mouse macrophage cell line RAW264.7 stimulated with indoxyl sulfate.** (A) Scheme of the cell stimulation and time points collected for quantitative proteomics using tandem mass tags (TMT). RAW264.7 cells were cultured with or without 1.0 mM indoxyl sulfate, and cells were collected at 0 minute (min), 15 min, 30 min, 1 hour (hr) and 3 hrs for subsequent proteolysis and labeling with one of ten TMT isobaric tags. (B) Workflow for protein selection based on protein profiles and corresponding pathway and network analysis.

# Supplemental Figure 5. The high resolution version of Figure 3B

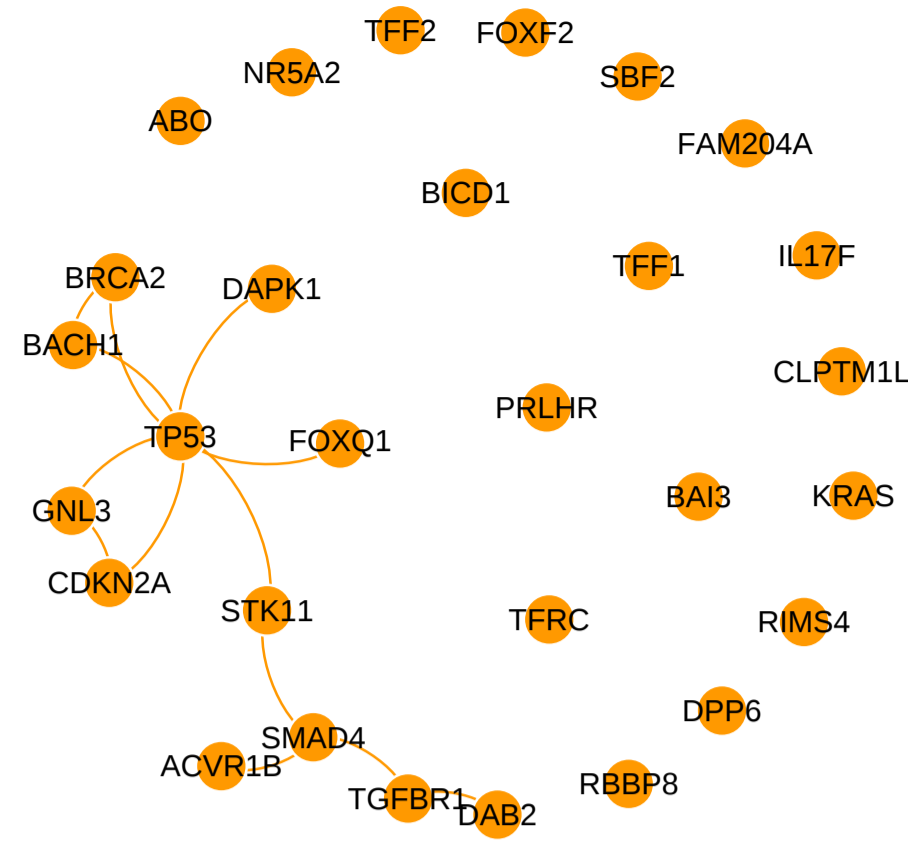




Aortic stenosis (p=0.32)

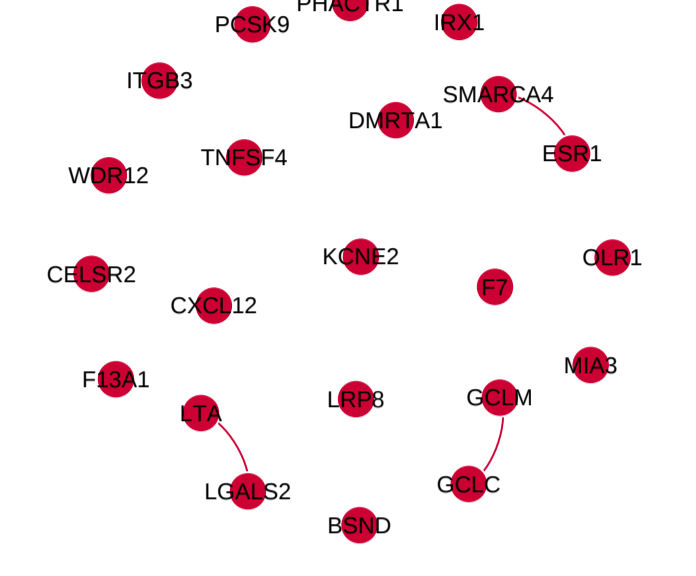
Takayasu's arteritis (p=0.79)

Pancreatic cancer (p=0.07)

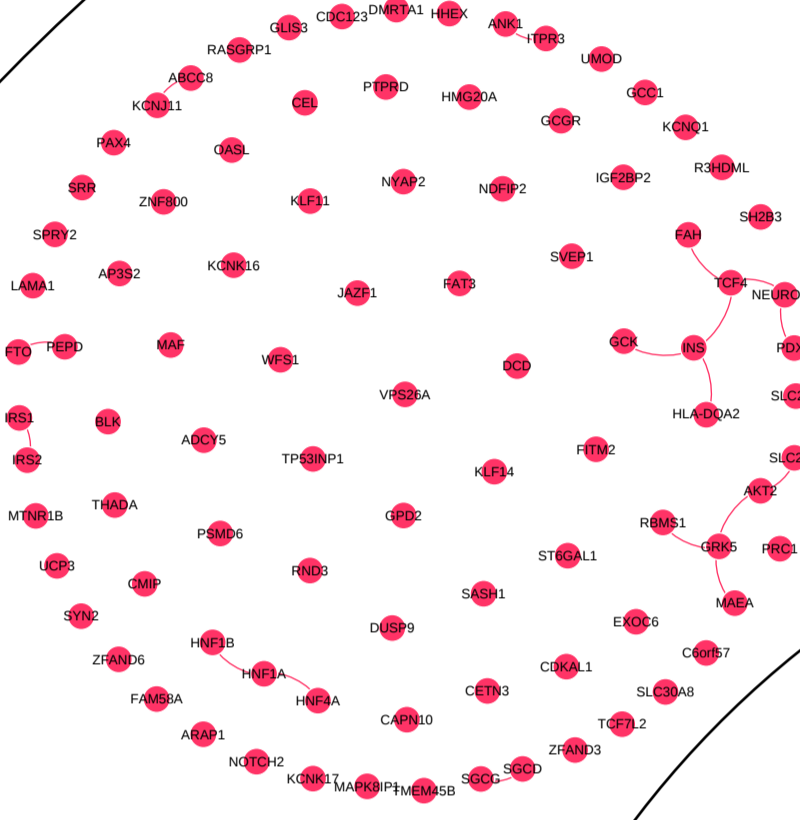


Diseases significantly close to Cluster 9 network

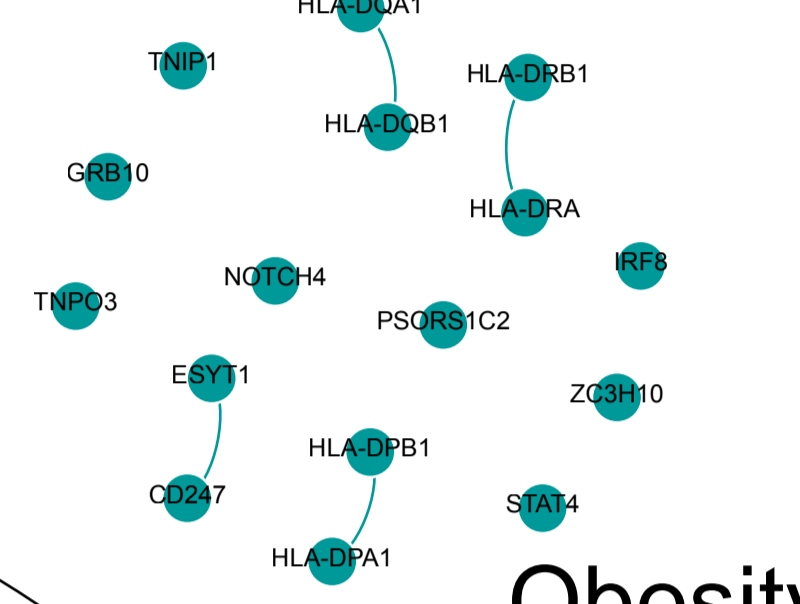
Myocardial infarction (p=0.05)



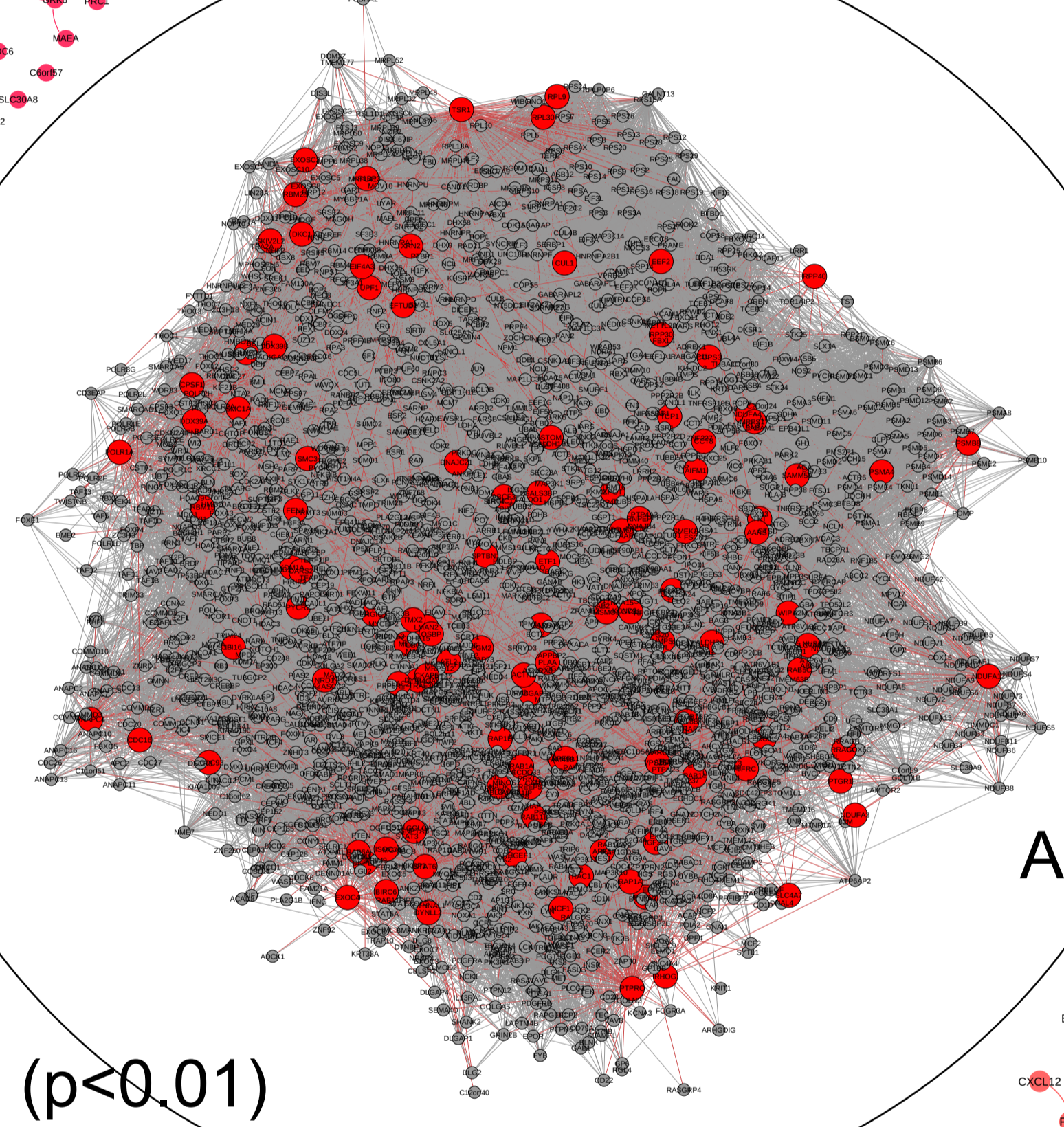
Type II diabetes (p=0.01)



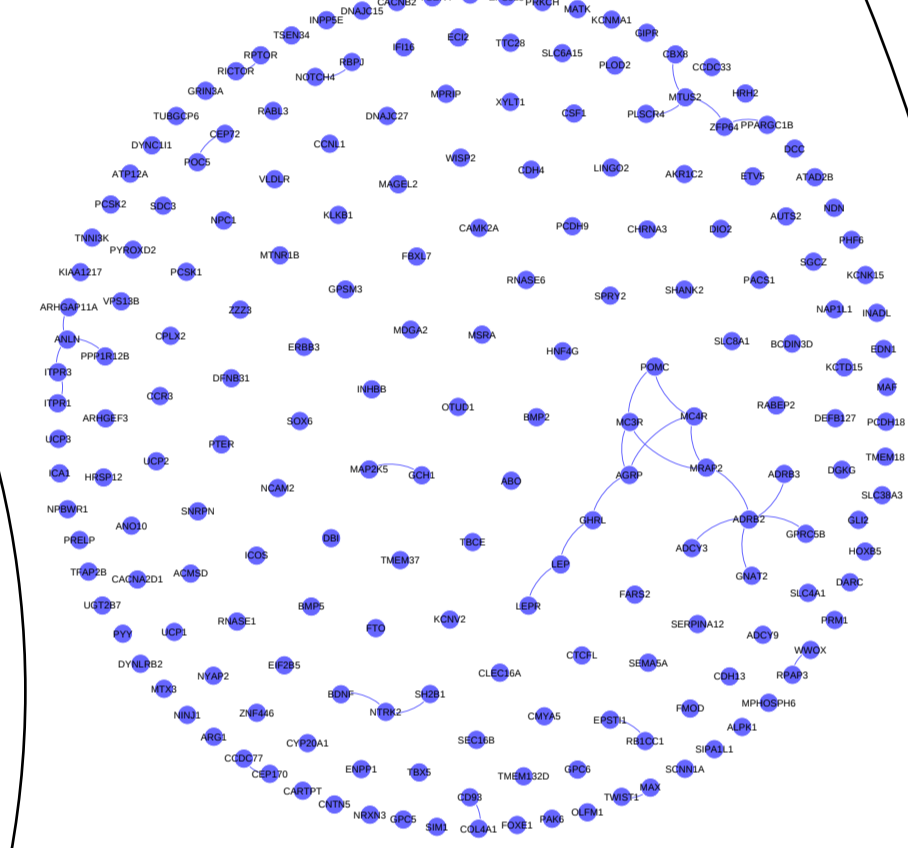
Scleroderma (p<0.01)



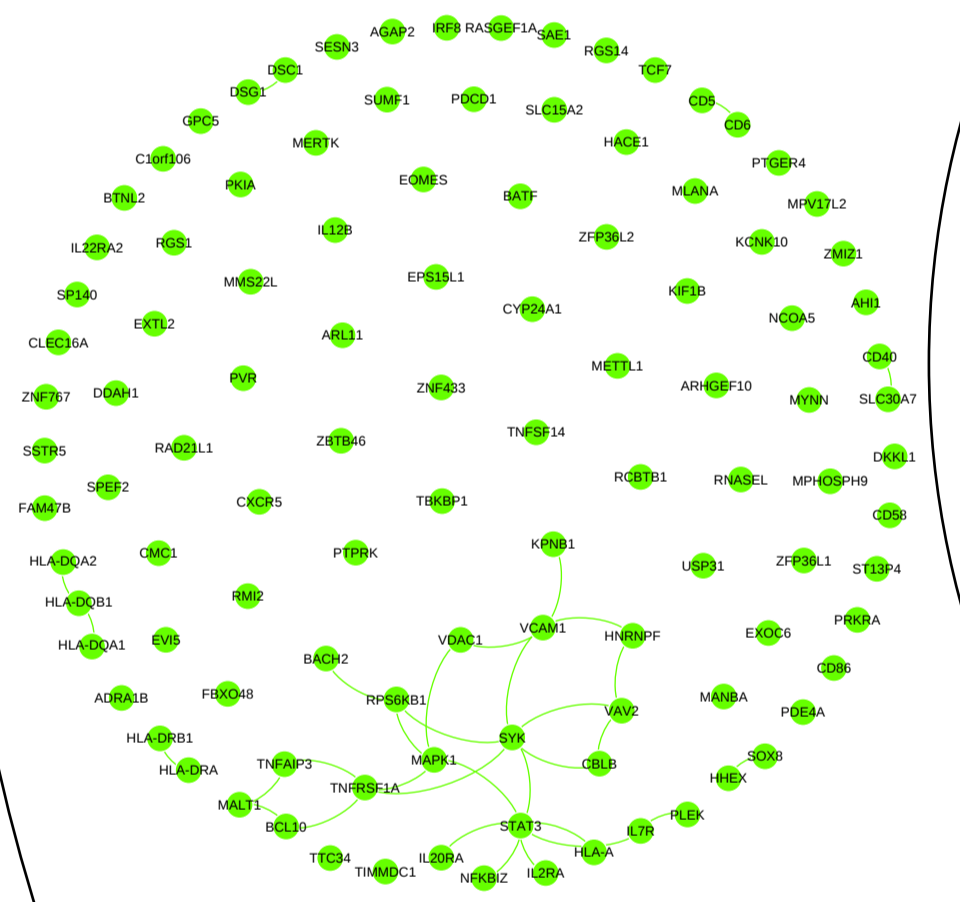
Cluster 9 subnetwork



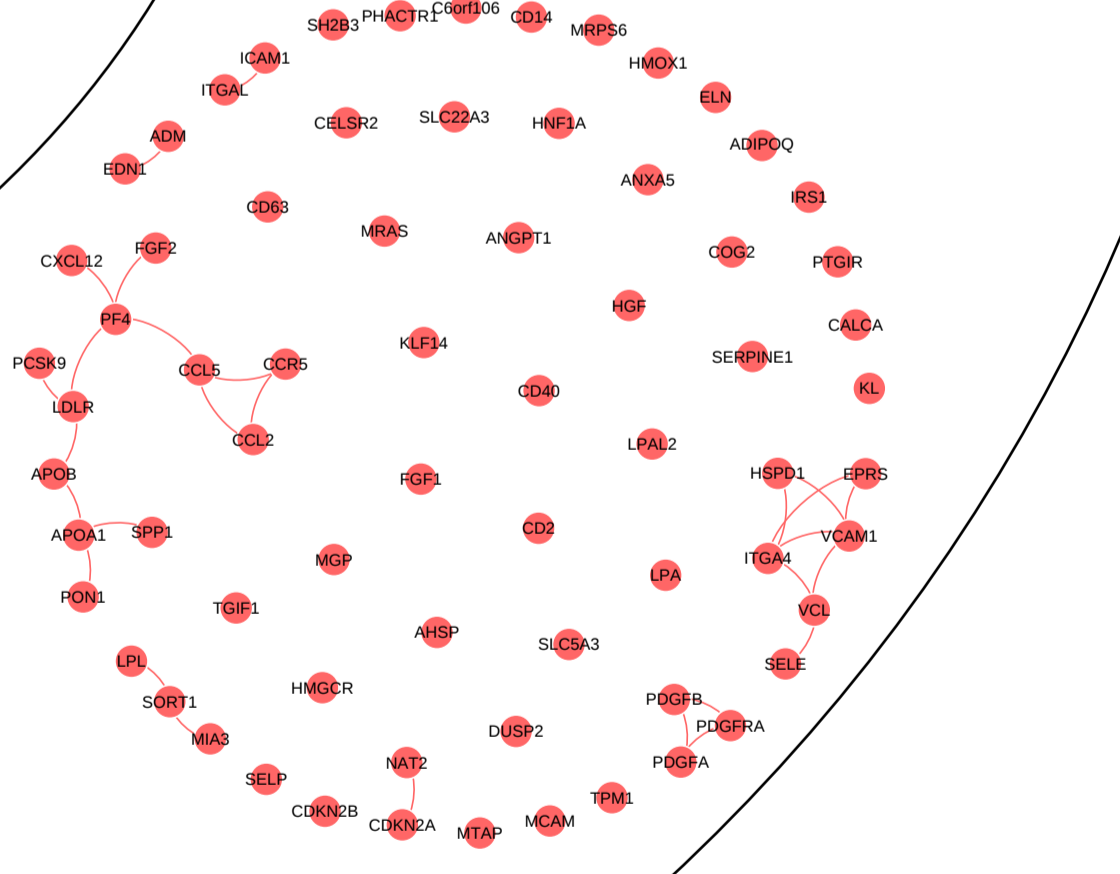
Obesity (p=0.02)



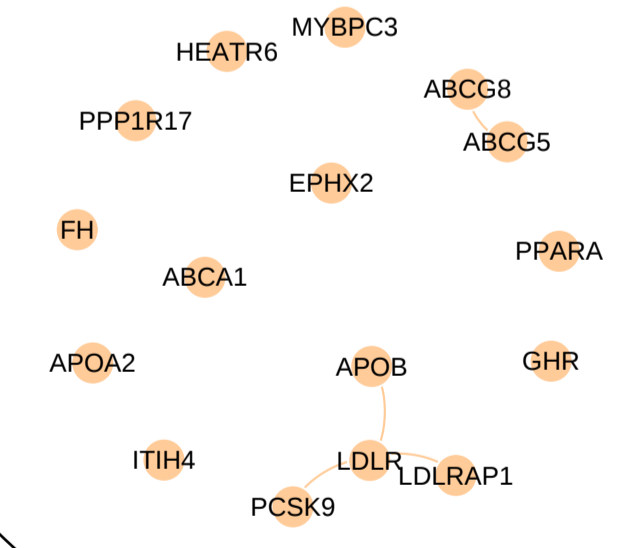
Multiple sclerosis (p<0.01)



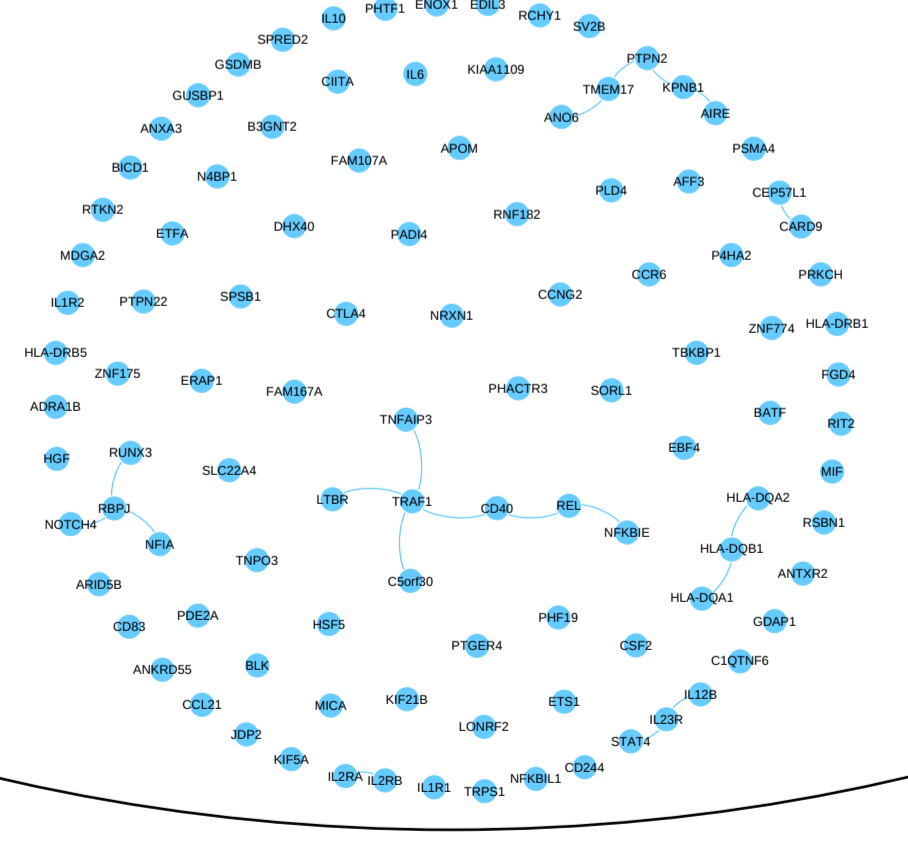
Atherosclerosis (p<0.01)



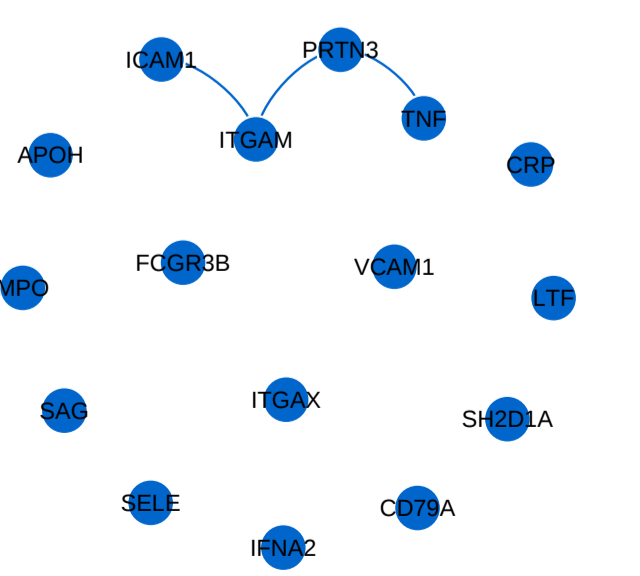
Hypercholesterolemia (p<0.01)



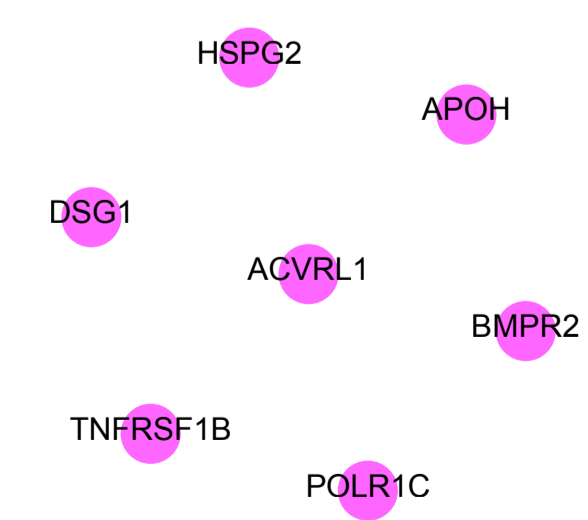
Rheumatoid arthritis (p=0.02)



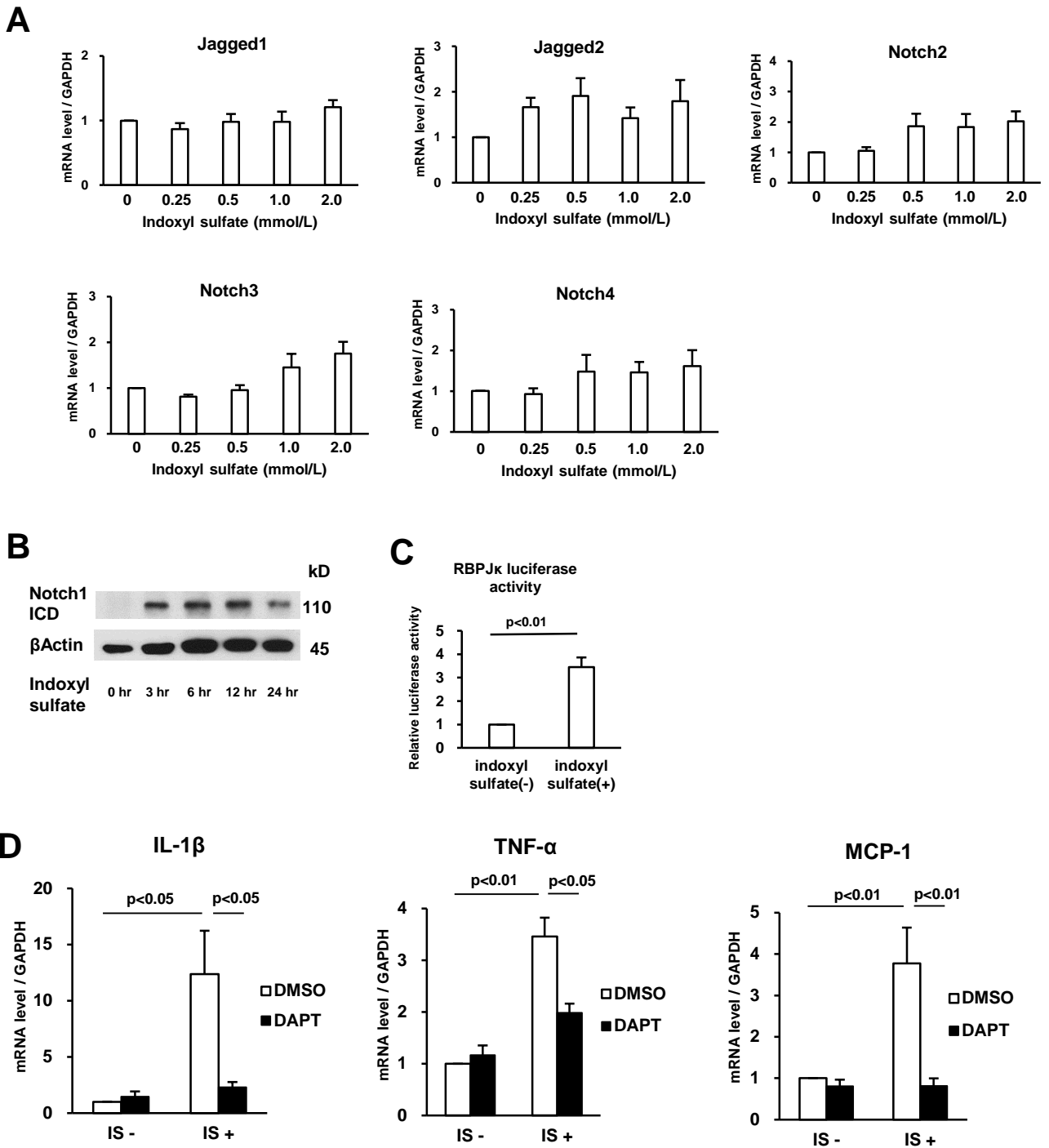
Vasculitis (p=0.08)



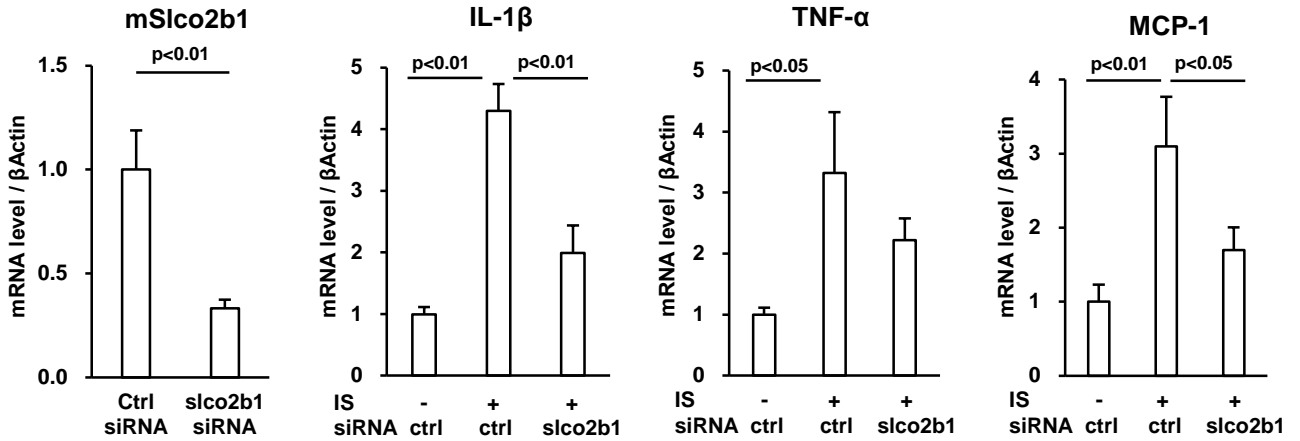
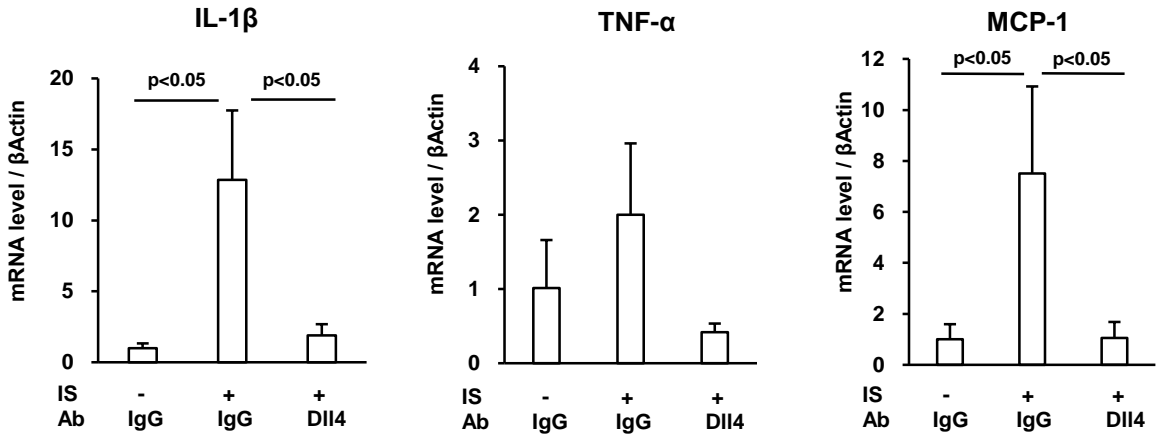
Mixed connective tissue disease (p=0.22)



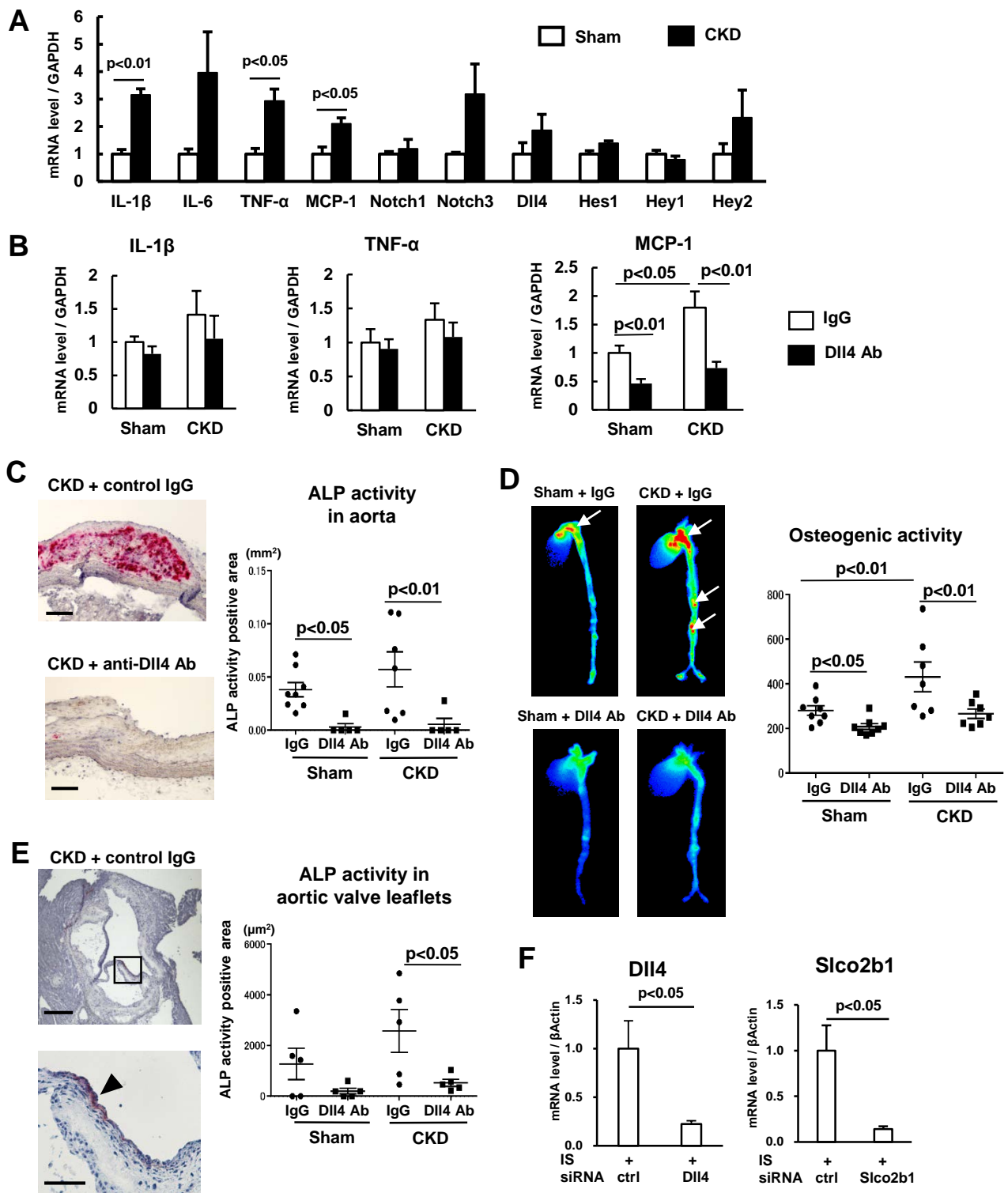




**Supplemental Figure 7. Notch signaling pathway stimulated with indoxyl sulfate in human primary macrophages.** (A) mRNA expression of other Notch pathway components was measured in human primary macrophages after stimulation with indoxyl sulfate for 3 hours (9 PBMC donors). P value was calculated by one-way ANOVA followed by Tukey's test, based on a comparison with 0 mmol/L indoxyl sulfate. Error bars indicate  $\pm$  SEM. (B) Notch1 intracellular domain (ICD) accumulation (Cleaved Notch1, Val1744) was measured in human primary macrophages by Western blotting after stimulation with 1.0 mmol/L indoxyl sulfate for 24 hours (hrs). These blots from one donor are representative of the 3 different macrophage donors. (C) RBP-Jk luciferase reporter activity increased in RAW264.7 macrophages after stimulation with 0.5 mmol/L indoxyl sulfate for 24 hrs. These data present cultures from 4 independent experiments. (D) mRNA expression was measured in human primary macrophages after pretreatment with 10  $\mu$ mol/L DAPT and stimulation with 0.5 mmol/L IS for 3 hours (9 donors). P value was calculated by two-way ANOVA followed by the Bonferroni test. Error bars indicate  $\pm$  SEM.

**A****B**

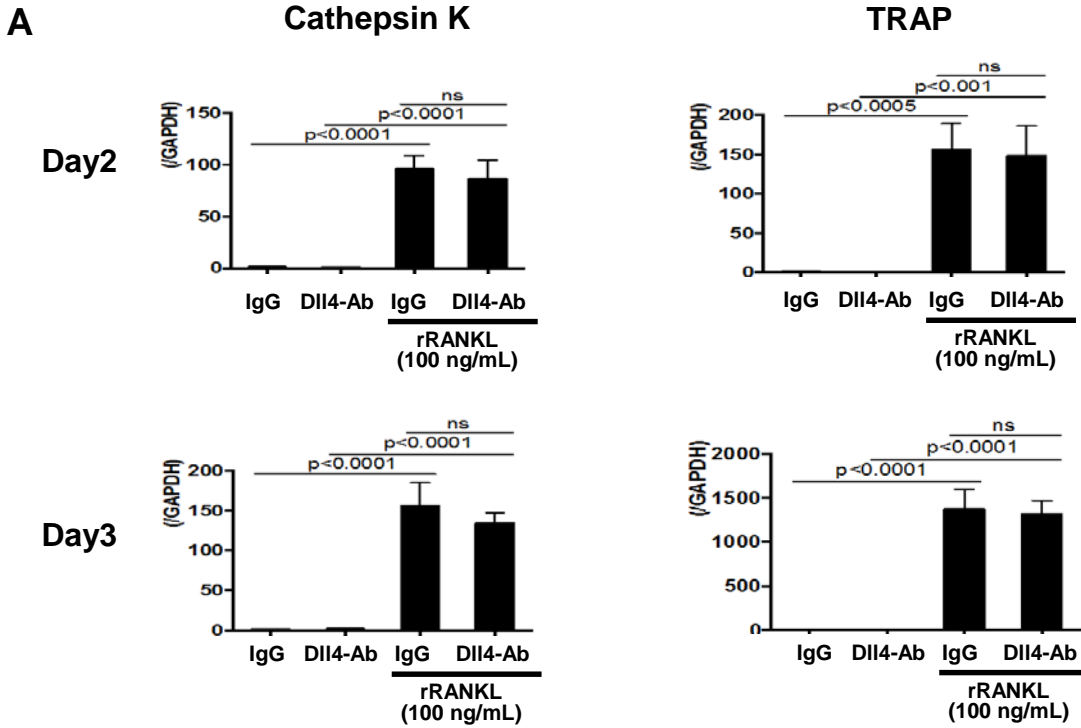
**Supplemental Figure 8. In vivo Slco2b1 siRNA delivery to macrophages and anti-DII4 antibody reduces pro-inflammatory gene expression induced by indoxyl sulfate in mouse macrophages.** Indoxyl sulfate of 100 mg/kg/day or PBS was intraperitoneally injected to C57BL/6 mice for a week. Peritoneal macrophages were collected and isolated by magnetic sorting for mRNA expression experiments. (A) Macrophage-targeted lipid nanoparticles (C12-200) containing control siRNA (Ctrl) or Slco2b1 siRNA were injected via tail vein twice a week (each n=8). (B) Hamster anti-mouse DII4 antibody (10  $\mu$ g/g per injection) or control IgG were also injected twice a week (each n=6). P value was calculated by unpaired Student's t-test or one-way ANOVA followed by Tukey's test. Error bars indicate  $\pm$  SEM.



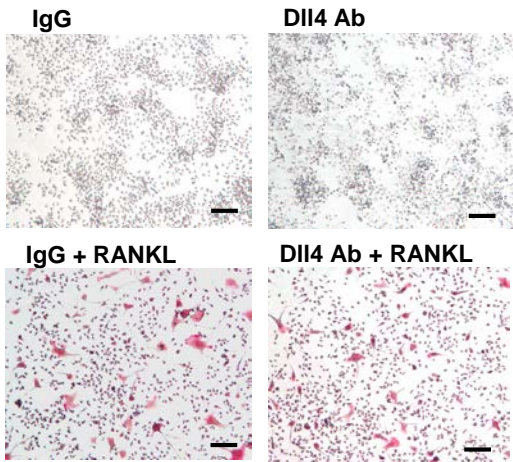
**Supplemental Figure 9. Pro-inflammatory gene expression and the effects of DII4 blockage in CKD mice.**

(A) The expression of pro-inflammatory molecules in splenic macrophages in sham-operated mice (control) and CKD mice (n=3) (B) The expression of pro-inflammatory molecules in aorta of sham-operated and CKD mice (n=5-9). (C) Staining for ALP activity in the aorta (each n=5 to 9). Scale bar = 100  $\mu$ m. (D) Molecular imaging of hydroxyapatite for osteogenic activity (see arrows) in the aorta (OsteoSense 680EX, Perkin Elmer, n=8). (E) ALP activity in aortic valves (each n=5). The lower panel is the corresponding lesion of the box indicated in the upper panel. Arrowhead shows the positive lesion of ALP activity in leaflet. Scale bar = 500  $\mu$ m (upper panel) and 200  $\mu$ m (lower panel). P value was calculated or two-way ANOVA followed by the Bonferroni test. Error bars indicate  $\pm$  SEM. (F) mRNA expression of DII4 and Slco2b1 in peritoneal macrophages of C57BL/6 mice in Figure 8.

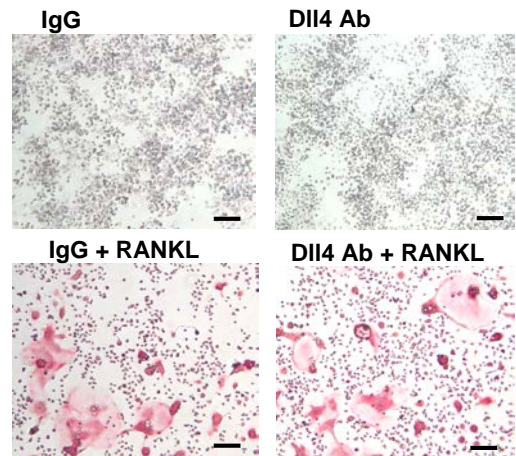




**B TRAP staining Day2**



**C TRAP staining Day3**



**Supplemental Figure 10. DII4 blockade does not inhibit osteoclast formation in RAW 264.7 cells.**

(A,B) RAW 264.7 cells were incubated with 50  $\mu$ g/mL of Hamster IgG or mouse DII4 Ab followed by stimulation with or without 100 ng/mL of recombinant mouse RANKL for 2 or 3 days. (A) mRNA expression of cathepsin K and TRAP was measured in RAW 264.7 cells after suppression by control IgG or DII4 Ab and stimulation with or without rRANKL (n=3). P value was calculated by one-way ANOVA followed by Tukey's test. Error bars indicate  $\pm$  SEM. (B,C) Osteoclast differentiation was evaluated by TRAP (tartrate-resistant acid phosphatase) staining after 2 or 3 days. Scale bar = 100  $\mu$ m. incubated with control IgG or DII4 Ab and rRANKL.

# Supplemental Table 1

Human primers for quantitative real time PCR

gene	Forward primer	Reverse primer
Human ABCG	5'-TCAGGGACCTTTCCTATTTCG-3'	5'-TTCCTTTCAGGAGGGTCTTGT-3'
Human ABCA1	5'-CCTGCTGTTGACAGGATTTG-3'	5'-TTTCCAGCCCCATTAAGTC-3'
Human IL-1 $\beta$	5'-GGACAAGCTGAGGAAGATGC-3'	5'-TCGTTATCCCATGTGTCAA-3'
Human TNF- $\alpha$	5'-GACAAGCCTGTAGCCCATGT-3'	5'-GAGGTACAGGCCCTCTGATG-3'
Human MCP-1	5'-CCCCAGTCACCTGCTGTTAT-3'	5'-AGATCTCCTTGGCCACAATG-3'
Human Notch1	5'-CGGGTCCACCAGTTTGAATG-3'	5'-GTTGTATTGGTTCGGCACCAT-3'
Human Notch2	5'-TGGTGGCAGAAGTCAAC-3'	5'-CTGCCAGTGAAGAGCAGAT-3'
Human Notch3	5'-CAATGCTGTGGATGAGCTTG-3'	5'-AAGTGGCTTCCACGTTGTTCC-3'
Human Notch4	5'-CCTCTCTGCAACCTTCCACT-3'	5'-GCCTCCATTGTGGCAAAG-3'
Human Dll1	5'-CTTCCCCTTCGGCTTCAC-3'	5'-GGGTTTTCTGTTGCGAGGT-3'
Human Dll4	5'-GAGGAGAGGAATGAATGTGTCA-3'	5'-GCTGAGCAGGGATGTCCA-3'
Human Jagged1	5'-GGCAACACCTTCAACCTCA-3'	5'-GCCTCCACAAGCAACGTATAG-3'
Human Jagged2	5'-TCATCCCCTTCCAGTTTCG-3'	5'-ATGCGACTCGCTCGAT-3'
Human Hes1	5'-TCAACACGACACCGGATAAA-3'	5'-TCAGCTGGCTCAGACTTTCA-3'
Human Hey1	5'-CGAGGTGGAGAAGGAGAGTG-3'	5'-CTGGGTACCAGCCTTCTCAG-3'
Human Hey2	5'-GAACAATTAATCGGGGCAAA-3'	5'-TCAAAAGCAGTTGGCACAAG-3'
Human SLCO2B1	5'-ATACCGCTACGACAACACCA-3'	5'-TGAGCAGTTGCCATTGGAG-3'
Human SLCO3A1	5'-ATCTTCCTGGTGTCCGAGTG-3'	5'-AGCGCTCTGCAGGTTGAA-3'
Human SLCO4A1	5'-TGGGAAAACCATCAGAGACC-3'	5'-ATGAACGTGGGGTTCTTCAG-3'
Human SLC22A20	5'-GGCGCAGTCCGTCTACAT-3'	5'-TGCAGGTAGGACCAGACCA-3'
Human SLCO1A2	5'-GGGGCATGCAGGATATATGA-3'	5'-TGGAAACAAAGCTTGATCCTCTT-3'
Human SLCO5A1	5'-CCCAAGTTCATCGAGTCACA-3'	5'-GCACTGGGGACGATAATAACC-3'
Human SLCO6A1	5'-AACACCCACTGTGGCAACTA-3'	5'-TCTAATGTGGAAACAATGACACCT-3'
Human SLC22A10	5'-CCATCATTGGTGGCCTTATT-3'	5'-TTTATGCCTTTTCTTGAGATTTT-3'
Human SLC22A11	5'-CGGTGCTGGACCTGTTCT-3'	5'-GCCCATAGGAGATCAATAGAGA-3'
Human MRC1	5'-CACCATCGAGGAATTGGACT-3'	5'-ACAATTCGTCATTTGGCTCA-3'
Human AMAC1	5'-ATGGCCCTCTGCTCCTGT-3'	5'-AATCTGCCAGGAGGTATAGACG-3'
Human IL-10	5'-GCAACCCAGGTAACCCTTAAA-3'	5'-GATGCCTTCAGCAGAGTGAA-3'
Human CD163	5'-GAAGATGCTGGCGTGACAT-3'	5'-GCTGCCTCCACCTCTAAGTC-3'
GAPDH	5'-TGGGTGTGAACCATGAGAAG-3'	5'-GCTAAGCAGTTGGTGGTGC-3'

## Supplemental Table 2

Human and mouse primers for semi-quantitative PCR

gene	Forward primer	Reverse primer
Human SLCO1A2	5'-TTTGCTTGCCAAGGAAGTGG-3'	5'-AAGGTGCTCACTGTGTTTGG-3'
Human SLCO2A1	5'-TGTATTTGGACCGGCTTTTCG-3'	5'-TTTGCTCCTATGGGCATTGC-3'
Human SLCO2B1	5'-TTGGGCATTTGCTGTGTTGG-3'	5'-AAGGCTGGCAAGTTCATTCC-3'
Human SLCO3A1	5'-TGCAACAGCAGCAATCTCAC-3'	5'-TGAAGCCCAACAAACGAAGG-3'
Human SLCO4A1	5'-AGAAGCTGCCACCTGTTTG-3'	5'-ACACAGGGCTGTAGTGTCTG-3'
Human SLCO5A1	5'-TGGTCAGCTGCTTTGACATC-3'	5'-GCGCGCAAATGAATAAAGCC-3'
Human SLCO6A1	5'-TGATAAGGTTCCGGCGTTTC-3'	5'-ACCAAACACCACACCTTGAC-3'
Human SLC22A6	5'-TGGTTTGCCACTAGCTTTGC-3'	5'-AAGAGAGGTTCCGACAATGGAC-3'
Human SLC22A7	5'-TGCGTCCACTTTCTTCTTCG-3'	5'-TGACAGCTAGCAGAAGCCATC-3'
Human SLC22A8	5'-TTGCTACCGTTTTGCCTAC-3'	5'-TTACGCCCATACCTGTTTGC-3'
Human SLC22A9	5'-AAATGCTCCACATGCCAAC-3'	5'-AAGCCCAGTGTGGCCAAAC-3'
Human SLC22A10	5'-TGTGTGACTTGTTCCGCAAC-3'	5'-TTTGGGCACAAACGTGTTGG-3'
Human SLC22A11	5'-AGAAACGGAGCCTTACAAGC-3'	5'-AAAAGGGTGCCGTTTGGTTG-3'
Human SLC22A20	5'-TCAGCTCCTTCAGTGCCTATTG-3'	5'-TGCAGACACTTGCAAACCTCG-3'
GAPDH	5'-TGGGTGTGAACCATGAGAAG-3'	5'-GCTAAGCAGTTGGTGGTGC-3'
Mouse Slco1a4	5'-TAAAGGCTCCTTGTCGAGATGG-3'	5'-ATTTTTGGTGGGGCATGCAC-3'
Mouse Slco1a5	5'-TGACAGACATGAAGCTCACAG-3'	5'-ACAACCTGAAAGCGTGGTTG-3'
Mouse Slco1a6	5'-ACAAGGCCAAGGAGGAAAAC-3'	5'-TTAAGCCGGCAATTGGAGTG-3'
Mouse Slco2a1	5'-TCTTCGTGCTTTGTCATGGC-3'	5'-TGAAAGTGGCTGCTGTTTCC-3'
Mouse Slco2b1	5'-TCGATACCACCTGTGTTCACTG-3'	5'-TTGCCATTGTTGGCAAACG-3'
Mouse Slco4a1	5'-TGCAACGCCATCTACTGTTG-3'	5'-TTTGCCGATCACTGACACAC-3'
Mouse Slco4c1	5'-AGCGCTGGTGTTTTCTTAC-3'	5'-TTGCTGTCCCTGGTAAATGC-3'
Mouse Slc22a6	5'-TTTCCTTTCCCGCACAATGG-3'	5'-ATGCTAGCCAAAGACATGCC-3'
Mouse Slc22a7	5'-AGCCTCGGTCAACTACATCATG-3'	5'-TTTGCGACACCCTTTCCATG-3'
Mouse Slc22a8	5'-TCAAAGGCTCTGAAGACACTCC-3'	5'-AACTTGGCGGGAATGTCAAC-3'
Mouse Slc22a12	5'-AGCAGGCTCATCACAAAGAC-3'	5'-AAGCTGCCATTGAGGTTGTC-3'
Mouse Slc22a13	5'-TGTCAGGCATCACAAGCATG-3'	5'-TGAAAAGGTCCAAGGCGTTC-3'
Mouse Slc22a19	5'-GCATCCCAGCCAATGTTCTTG-3'	5'-ATGGTGTCACTTTGGCAACC-3'
Mouse Slco1a1	5'-AGGTTGCAACACAAGAAGGC-3'	5'-TGCGTTGGCTTTAAGGTCTG-3'
Mouse Slco1c1	5'-TTGCAGCTGTTCTTTCTGG-3'	5'-AGCCCAATGACAAAGTTGGC-3'
Mouse Slco3a1	5'-ACAACGTGAATGCCAGACG-3'	5'-AAAGGACTTGAGCGCAATGG-3'
βactin	5'-CCTGAGCGCAAGTACTCTGTGT-3'	5'-GCTGATCCACATCTGCTGGAA-3'

### Supplemental Table 3

Mouse primers for quantitative real time PCR

gene	Forward primer	Reverse primer
Mouse IL-1 $\beta$	5'-GCCCATCCTCTGTGACTCAT-3'	5'-AGGCCACAGGTATTTTGTCG-3'
Mouse IL-6	5'-AGTTGCCTTCTTGGGACTGA-3'	5'-TCCACGATTTCCAGAGAAC-3'
Mouse TNF- $\alpha$	5'-AGCCCCCAGTCTGTATCCTT-3'	5'-CTCCCTTTGCAGAACTCAGG-3'
Mouse MCP-1	5'-AGGTCCCTGTCATGCTTCTG-3'	5'-TCTGGACCCATTCTTCTTG-3'
Mouse Notch1	5'-TGAGACTGCCAAAGTGTTGC-3'	5'-GTGGGAGACAGAGTGGGTGT-3'
Mouse Notch3	5'-GGGTCTTGTCTGCTCAAAGC-3'	5'-GGCTGAGCCAAGAGAACAAC-3'
Mouse Dll4	5'-ACCTTTGGCAATGTCTCCAC-3'	5'-GTTTCCTGGCGAAGTCTCTG-3'
Mouse Hes1	5'-ACACCGGACAAACCAAAGAC-3'	5'-ATGCCGGGAGCTATCTTTCT-3'
Mouse Hey1	5'-GGTACCCAGTGCCTTTGAGA-3'	5'-ATGCTCAGATAACGGGCAAC-3'
Mouse Hey2	5'-GTTCCGCTAGGCGACAGTAG-3'	5'-TGCCCAGGGTAATTGTTCTC-3'
Mouse Slco2b1	5'-TTCAGGCGGAAGGTCTTG-3'	5'-CCTGTTTCTTTAAAGGCTCGTG-3'
$\beta$ actin	5'-CCTGAGCGCAAGTACTCTGTGT-3'	5'-GCTGATCCACATCTGCTGGAA-3'
Mouse CathepsinK	5'-GAAGAAGACTCACCAGAAGCAG-3'	5'-TCCAGTTATGGGCAGAGATT-3'
Mouse TRAP	5'-GCAACATCCCCTGGTATGTG-3'	5'-GCAAACGGTAGTAAGGGCTG-3'
GAPDH	5'-AGGTCGGTGTGAACGGATTTG-3'	5'-TGTAGACCATGTAGTTGAGGTCA-3'

## Supplemental Table 4

### Serum biochemistry and blood pressure

	Sham IgG	Sham DII4 Ab	CKD IgG	CKD DII4 Ab
Serum urea (mmol/L)	20.9±1.5 <sup>#</sup>	19.5±1.9 <sup>#</sup>	44.4±1.2 <sup>*</sup>	47.9±4.1 <sup>*</sup>
Serum creatinine (µmol/L)	15±4 <sup>#</sup>	11±4 <sup>#</sup>	37±6 <sup>*</sup>	38±7 <sup>*</sup>
Total cholesterol (mmol/L)	24.6 ±2.6	28.2±2.2	26.3±3.5	28.3±3.3
Triglyceride (mmol/L)	3.09±0.35	3.57±0.57	2.55±0.38	3.29±0.46
Phosphate (mmol/L)	2.58±0.13 <sup>#</sup>	2.84±0.23 <sup>#</sup>	4.29±0.29 <sup>*</sup>	4.55±0.23 <sup>*</sup>
Calcium (mmol/L)	2.22±0.12	2.32±0.15	2.02±0.05	2.12±0.05
Indoxyl sulfate (µg/mL)	0.57±0.19 <sup>#</sup>	0.54±0.19 <sup>#</sup>	14.14±3.17 <sup>*</sup>	11.70±2.73 <sup>*</sup>
Systemic pressure (mmHg)	119.8±4.3	122.6±3.8	122.0±2.5	118.5±4.0
Diastolic pressure (mmHg)	80.4±5.4	77.3±4.0	81.6±5.7	83.1±3.3

N=10, each group.

\*indicates significance between Sham IgG and other groups.

<sup>#</sup>indicates significance between CKD IgG and other groups.

The statistical analysis was calculated by two-way ANOVA followed by the Bonferroni test.

The values indicate mean ± SEM.